Settlement of the Kansai International Airport Islands

by

Gholamreza Mesri

Ralph B. Peck Professor of Civil Engineering

University of Illinois at Urbana-Champaign, Urbana, Illinois, U.S.A.

Jason Funk

Shannon & Wilson, Inc., Seattle, Washington, U.S.A.

GeoVirginia Conference

Williamsburg, Virginia

April 28, 2015

JAPAN
Sea of Okhotsk
Sea of Japan
Pacific Ocean
HOKKAIDO
HONSHU
KYUSHU
SHIKOKU
NANSEI(Southwest) ISLANDS (Okinawa)
Japan National Tourist Org map
Major Cities
Shinkansen (JR)
Japan Railways (JR)
Additions by Randy Johnson
http://ease.com/~randyj/japan.htm
Wakkanai
Etorofu isl.
Shiretoko pen.
Abashiri
Kunashiri isl.
Asahikawa
Shari
Rausu
Mt. Asahidake
L. Mashu
L. Akan
Otaru
Furano
Nemuro
SAPPORO
Obihiro
L. Shikotsu
Chitose
Kushiro
L. Toya
Tomakomai
Noboribetsu
Muroran
Hakodate
AOMORI
Hirosaki
Hachinohe
L. Towada
AKITA
MORIOKA
Hanamaki
Hiraizumi
Sado isl.
YAMAGATA
NIIGATA
SENDAI
Mt. Zao
Mt. Bandai
FUKUSHIMA
L. Inawashiro
Wajima
Notto pen.
Itoigawa
TOYAMA
KANAZAWA
NAGANO
L. Chuzenji
Nikko
Shirakawa-go
Matsumoto
UTSUNOMIYA
Tojimbo
Oki isl.
FUKUI
Takayama
MAEBASHI
MITO
Tango pen
Wakasa Bay
Kamikochi
MATSUE
TOTTORI
URAWA
Idzumo
Sekigane
Izushi
GIFU
Magome
KOFU
Hikawa
TOKYO
L. Biwa
Fuji Five Lakes
CHIBA
Tsushima isl.
KYOTO
Maibara
Mt. Fuji
NAGOYA
YOKOHAMA
Hagi
HIROSHIMA
OKAYAMA
KOBE
OTSU
SHIZUOKA
Hakone
Atami
Ito
YAMAGUCHI
Miyajima
Kurashiki
Himeji
NARA
TSU
Shimonoseki
Inland Sea
Awaji isl.
OSAKA
Asuka
Ise
Hamamatsu
Izu pen.
FUKUOKA (Hakata)
Kokura
Imabari
TAKAMATSU
Toba
Karatsu
MATSUYAMA
TOKUSHIMA
WAKAYAMA
Hongu
SAGA
Beppu
OITA
KOCHI
Shirahama
Shingu
Uwajima
NAGASAKI
KUMAMOTO
Mt. Aso
Nobeoka
MIYAZAKI
KAGOSHIMA
Ibusuki
N
Naze
NANSEI (Southwest) ISLANDS
Okinawa
NAHA
Pacific Ocean
100
200 Mile
300km


Miki
Takarazuka
Airport
大阪国際空港
Ibara
Takasago
Kakogawa
Itami
Nishinomiya
Amagasaki
Suita
Kakogawa
River
加古川
Ashiya
阪神電鉄本線
Osaka
Kobe
Osaka Bay
大阪湾
Kobe Airport
神戸空港
山陽新幹線
Akashi
山陽本線
Yamato
River
大和川
Osaka
Sakaisenboku
Port
堺泉北港
Sakai
Takaishi
Osaka Bay
大阪湾
Tondabay
Izumiotsu
Kansai
International
Airport
関西国際空港
Izumi
Kawachinagan
Awaji
Awaji Island
淡路島
Kishiwada
Izumisano
Osaka Bay
大阪湾
Hannan
Hanwa Expy
Sumoto
Hashim
inamiawaji
Kinokawa

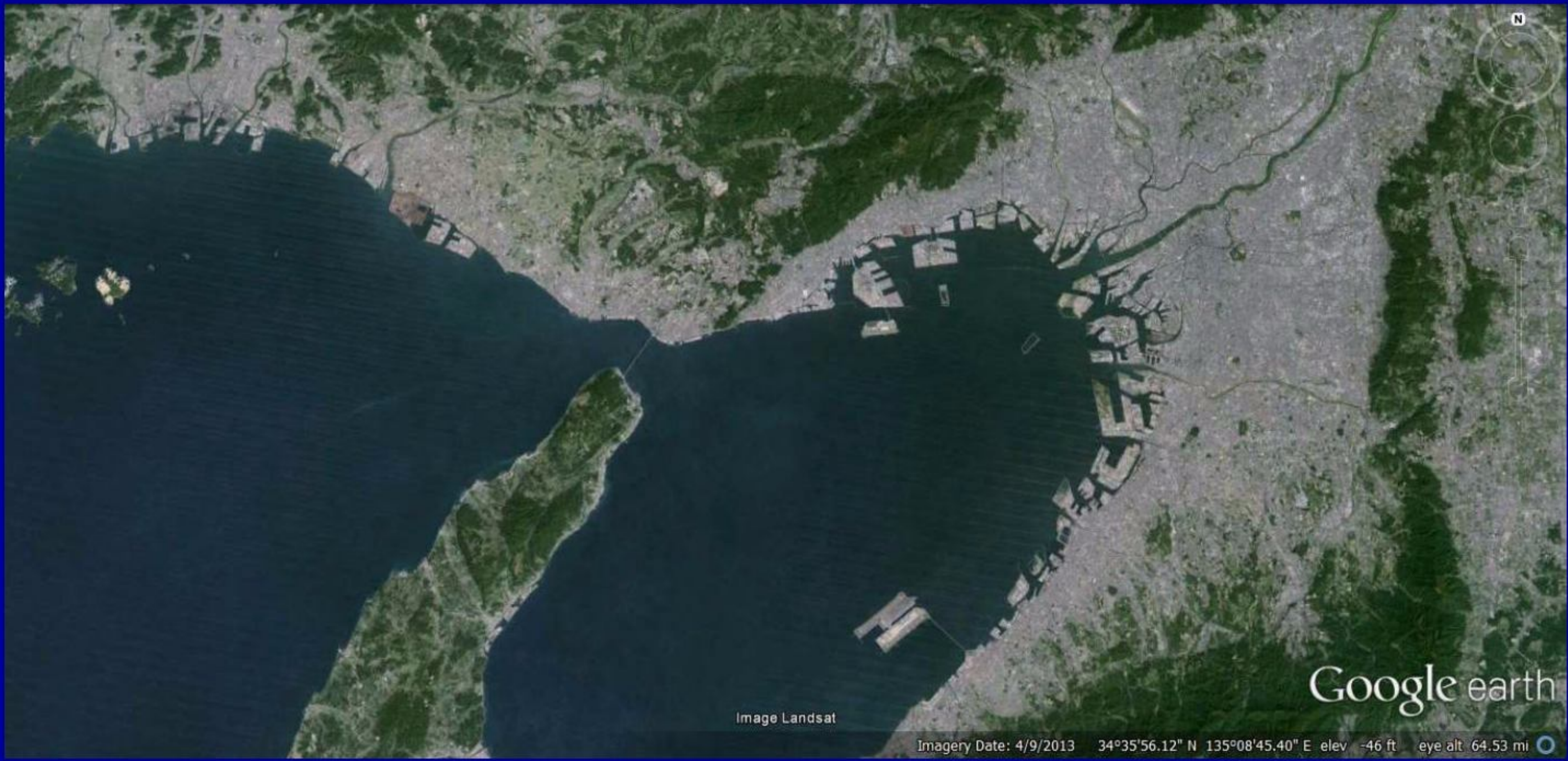
Google earth
Image Landsat
Imagery Date: 4/9/2013 34°35'56.12" N 135°08'45.40" E elev -46 ft eye alt 64.53 mi

Settlement of the Kansai International Airport Islands

1. Introduction
2. Offshore Reclamation History of Japan
3. Geology of Osaka Bay
4. Construction of the Kansai Airport Islands

Settlement of the Kansai International Airport Islands (cont.)

5. ILLICON Procedure for Settlement Analysis

   Permeability of Osaka Bay Sediments

   Compressibility of Osaka Bay Clay Layers

   Hydrodynamic Equation

   Constitutive Equation

Settlement of the Kansai International Airport Islands (cont.)

6. Observed and Computed Settlements

   Holocene Layer, Airport Islands I and II

   Pleistocene Layers, Airport Islands I and II

   Seafloor Settlement

7. Conclusions

Introduction

- Kansai International Airport Island Ⅰ and Island Ⅱ, located 5 km off the Senshu Coast in Osaka Bay, Southwest Japan, were constructed as a part of an effort to globalize the Kansai Region.

Introduction (cont.)

- Construction of Island Ⅰ began in 1987 and the Island Ⅰ runway began operation in 1994.
- Construction of Island Ⅱ began in 1999 and the Island Ⅱ runway began operation in 2007.

Introduction (cont.)

- The Kansai Airport project has been viewed as an engineering marvel.
- The American Society of Civil Engineers named the airport one of the "Civil Engineering Monuments of the Millennium."

Introduction (cont.)

- Airport Island I is 511 ha in 18 m deep seawater; height of reclamation fill above seafloor is 37 m
- Airport Island II is 545 ha in 20 m deep seawater; height of reclamation fill above seafloor is 43 m.

Offshore Reclamation History of Japan

- Japan’s extensive reclamation history stems from a need for additional land in coastal areas.
- Reclamation has taken place in Osaka Bay at least as early as the Edo Era (1600 – 1867) when it was used for rice cultivation.

Reclamation History (cont.)

- Reclamation projects in Osaka Bay include:

  Sakishima, 2002 ha

  Maishima, 224 ha

  Yumeshima, 391 ha

  Island offshore of Yumeshima, 300 ha

  Port Island, 436 ha

  Rokko Island, 580 ha

Geology of Osaka Bay

- Osaka Bay in Southwest Japan is bordered by the Rokko Mountains to the north, the Ikoma and Kongo Mountains to the east and the Izumi Mountains to the south.
- Osaka Basin formed as a result of crustal movements that started in the middle Miocene Epoch, caused by the subduction of the Philippine Sea Plate beneath the Eurasian Plate.

Geology of Osaka Bay (cont.)

- The subseabed sediments in Osaka Bay are a result of changes of global climate, sea level fluctuations as well as volcanic activity that occurred during the late Cenozoic Era.
- The maximum depth to bedrock in Osaka Bay is more than 3000 m near the center of the Bay.

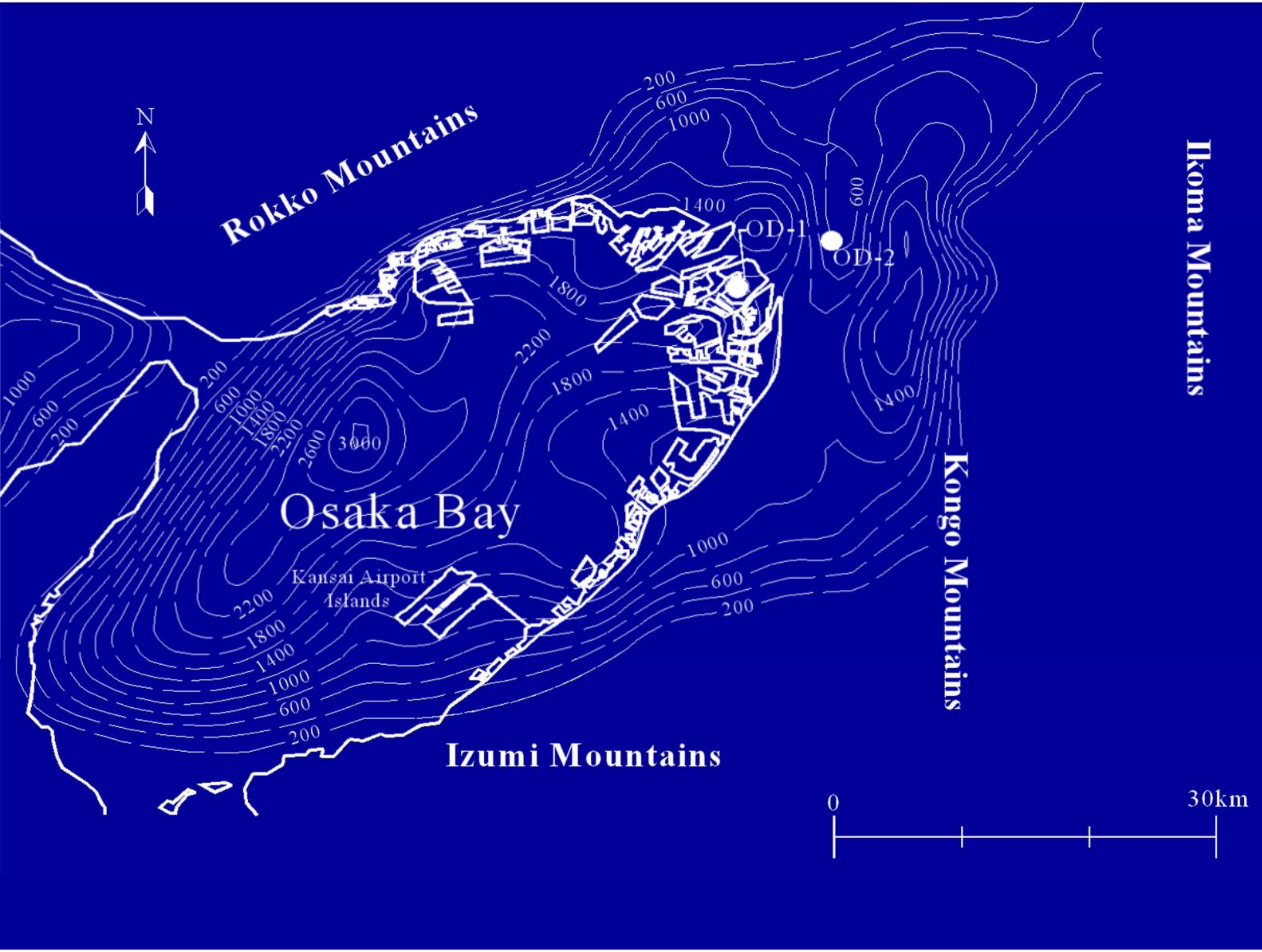

N
Rokko Mountains
Ikoma Mountains
Kongo Mountains
Izumi Mountains
Osaka Bay
Kansai Airport Islands
OD-1
OD-2
200
600
1000
1400
1800
2200
2600
3000
0
30km

Geology of Osaka Bay (cont.)

- Osaka Basin began to subside and accumulate sediments at the close of the Pliocene.
- The profile includes Pleistocene marine clay layers Ma 0 through Ma 12 and Holocene marine clay layer Ma 13.
- Marine clay layers alternate with marine and fresh water sand layers Ds 1 through Ds 10.

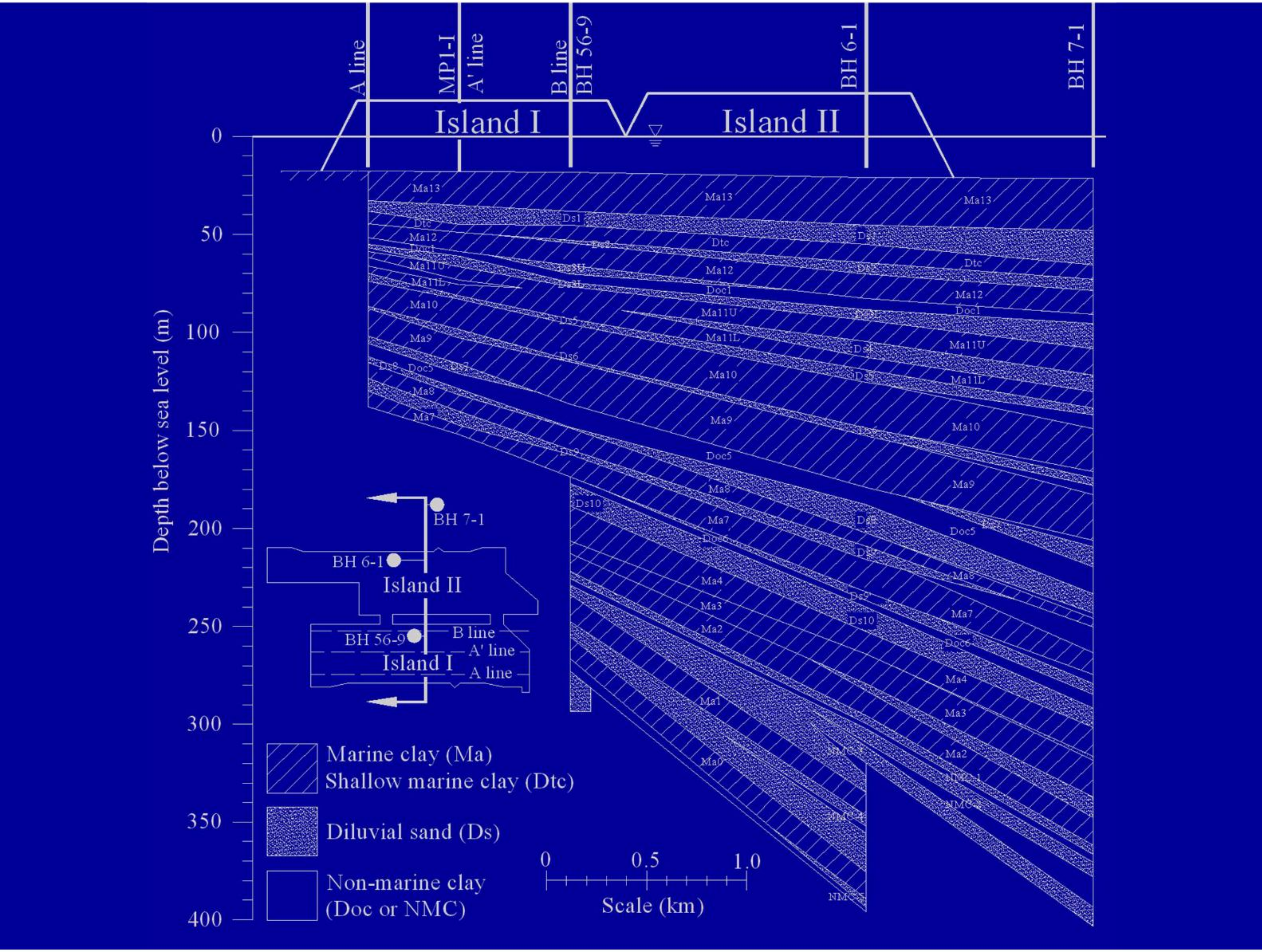

A line
MP1-I
A' line
B line
BH 56-9
BH 6-1
BH 7-1
Island I
Island II
Depth below sea level (m)
0
50
100
150
200
250
300
350
400
Ma13
Ds1
Dtc
Ma12
Doc1
Ma11U
Ma11L
Ma10
Ma9
Ds5
Ds6
Ds8
Doc5
Ds7
Ma8
Ma7
Ds9
Ds10
Doc6
Ma6
Ma4
Ma3
Ma2
Ma1
Ma0
BH 7-1
BH 6-1
Island II
BH 56-9
B line
A' line
Island I
A line
Marine clay (Ma)
Shallow marine clay (Dtc)
Diluvial sand (Ds)
Non-marine clay
(Doc or NMC)
0
0.5
1.0
Scale (km)

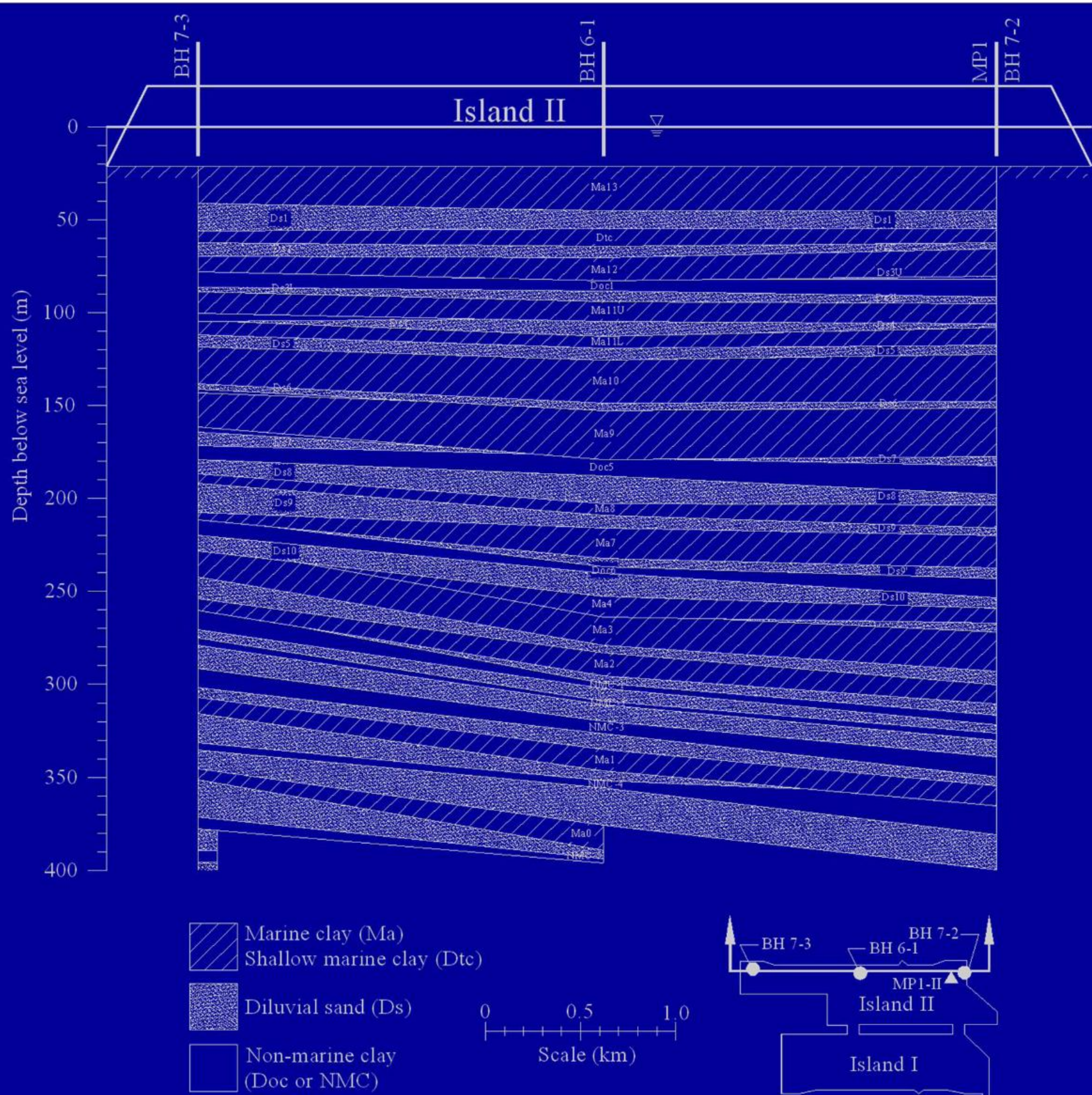

BH 7-3
BH 6-1
MP1
BH 7-2
Island II
0
50
100
150
200
250
300
350
400
Depth below sea level (m)
Ma13
Ds1
Dtc
Ma12
Ds3U
Doc1
Ma11U
Ma11L
Ds5
Ma10
Ma9
Ds7
Doc5
Ds8
Ds9
Ma8
Ma7
Ds10
Ma4
Ma3
Ma2
NMC-3
Ma1
NMC-4
Ma0
Marine clay (Ma)
Shallow marine clay (Dtc)
Diluvial sand (Ds)
Non-marine clay
(Doc or NMC)
0
0.5
1.0
Scale (km)
BH 7-3
BH 6-1
BH 7-2
MP1-II
Island II
Island I

Geology of Osaka Bay (cont.)

- The depositional environment, lateral continuity and age of the Osaka Bay sediments are constrained by more than 50 volcanic ash layers.
- At the Kansai Airport site:

  1 million YBP ash in between Ma 1 and Ma 2

  0.85 million YBP ash in lower portion of Ma 3

  0.30 million YBP ash in Ma 10

  0.23 million YBP ash in Ma 11

  20 thousand YBP ash in Ds 1

  6.3 thousand YBP ash in Ma 13

Geology of Osaka Bay (cont.)

- The subseabed investigation for the Kansai International Airport project began in 1977.
- Sixty-three borings were made to seabed depths ranging from 100 to 200 m, and six borings were made to seabed depth of 400 m, four in 1994 and 1995.

Construction of the Kansai Airport Islands

- In April 1968, the Ministry of Transportation of Japan began surveying 2 onshore and 6 offshore sites for airport construction.
- It was decided in 1974 that an airport 5 km off the coast of Senshu would avoid noise-related problems and land acquisition disputes.

Construction of the Kansai Airport Islands (cont.)

- The construction of each airport island consisted of four stages:

1. Installation of vertical sand drains in the Ma 13 clay layer following placement of a 1.5 m thick sand blanket on the sea floor
2. Construction of the seawall around the reclamation site
3. Reclamation of the airport island
4. Construction of airport facilities

Construction of the Kansai Airport Islands (cont.)

- Forty centimeter diameter displacement type vertical sand drains were installed, on a 2.5 m square pattern, to fully penetrate the Holocene marine clay layer Ma 13 and form a drainage connection to the overlying sand blanket and under lying sand layer Ds 1.
- Approximately 1 million sand drains were installed for Island I construction and 1.2 million sand drains were installed for Island II construction.

Construction of the Kansai Airport Islands (cont.)

- The reclamation fill with a maximum particle size of 300 mm was obtained from Misaki, Kada, Tsuna, and Sumoto, located 10 to 30 Km from the Kansai Airport site.
- Reclamation started with large hopper barges and continued as seawater depth decreased with smaller hopper barges, box barges, and shovel and dump trucks.

Construction of the Kansai Airport Islands (cont.)

- Above sea level, to reach the final reclamation height, the fill was placed in 60 cm lifts with 8 passes of a vibratory roller for each lift.

ILLICON Procedure for Settlement Analysis

- The Darcy law of flow
- Uniqueness of end-of-primary (EOP) void ratio-effective vertical stress relationship
- The C_{α}/C_c law of compressibility

ILLICON Procedure for Settlement Analysis (cont.)

- Vertical compression
- Vertical and horizontal water flow
- 22 clay layers 2.4 to 26.4 m thick
- 19 sand layers 2 to 15 m thick
- 39 clay sublayers

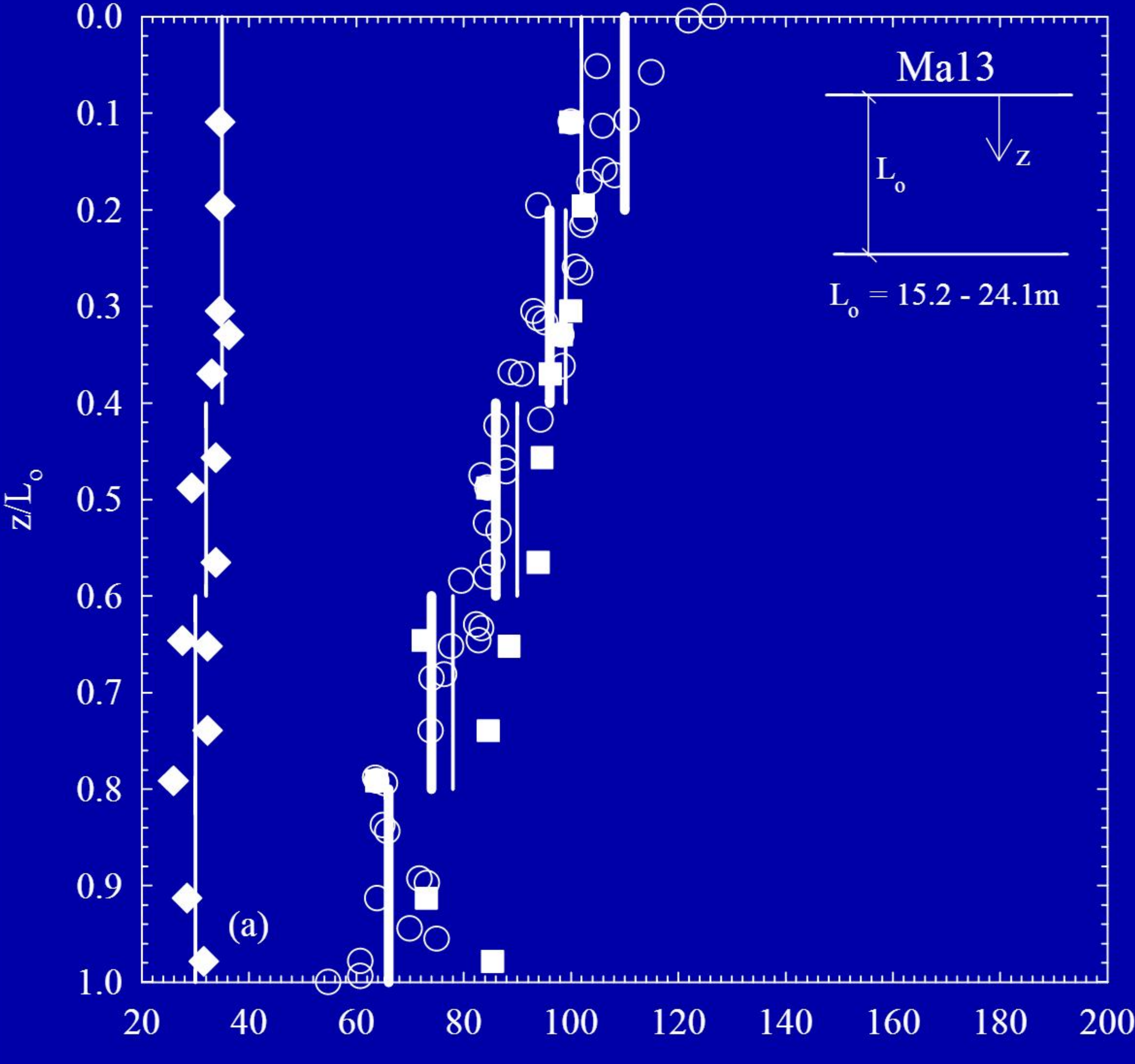

Ma13
z
L_o
L_o = 15.2 - 24.1m
(a)
z/L_o
Water content (%)
0.0
0.1
0.2
0.3
0.4
0.5
0.6
0.7
0.8
0.9
1.0
20
40
60
80
100
120
140
160
180
200

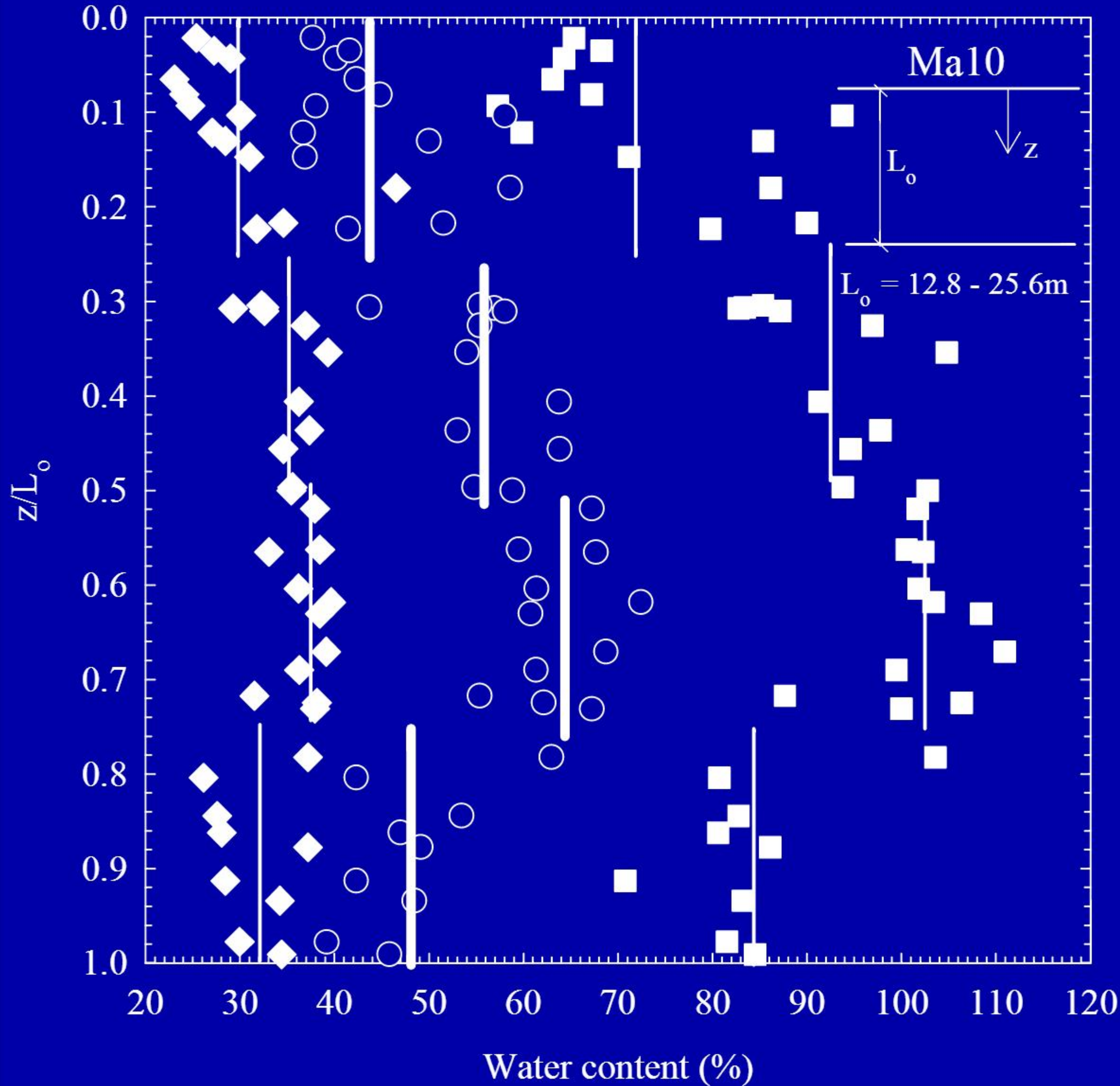
Ma10
z
L_o
L_o = 12.8 - 25.6m
z/L_o
0.0
0.1
0.2
0.3
0.4
0.5
0.6
0.7
0.8
0.9
1.0
20
30
40
50
60
70
80
90
100
110
120
Water content (%)

Permeability of Osaka Bay Sediments

- Clay sublayers

$$k_{vo}(\mathrm{m/s}) = 6.5 \times 10^{-11}\left(\frac{e_o/CF}{A_c + 1}\right)^4$$

$$C_k = 0.5\, e_o$$

Permeability of Osaka Bay Sediments (cont.)

- The permeability of the sand layers was back-calculated using the observed settlements and porewater pressures.
- Sand layers Ds 1 and Ds 10 were assumed to be freely draining.
- Permeability of sand layers Ds 2 to Ds 9 were in the range of 10^{-7} to 10^{-4} m/s.

Compressibility of Osaka Bay Clay Layers

- EOP $e - \log \sigma'_v$ relationship for each sublayer constructed using e_o, σ'_{vo}, C_r/C_c, σ'_p/σ'_{vo} and C'_c versus $\log \sigma'_v/\sigma'_p$ data.

Compressibility of Osaka Bay Clay Layers (cont.)

- The values of σ'_p/σ'_{vo} for the clay layers at Kansai Airport site were obtained from incremental loading and constant rate of strain oedometer tests.

Compressibility of Osaka Bay Clay Layers (cont.)

- $\dot{\varepsilon}_p = \dfrac{k_{vo}}{2^{C_c/C_k} H^2} \dfrac{\sigma'_p}{\gamma_w} \dfrac{C_\alpha}{C_c}$

- $\dfrac{[\sigma'_p]_{\dot{\varepsilon}_p}}{[\sigma'_p]_{\dot{\varepsilon}_I}} = \left(\dfrac{\dot{\varepsilon}_p}{\dot{\varepsilon}_I}\right)^{C_\alpha/C_c}$

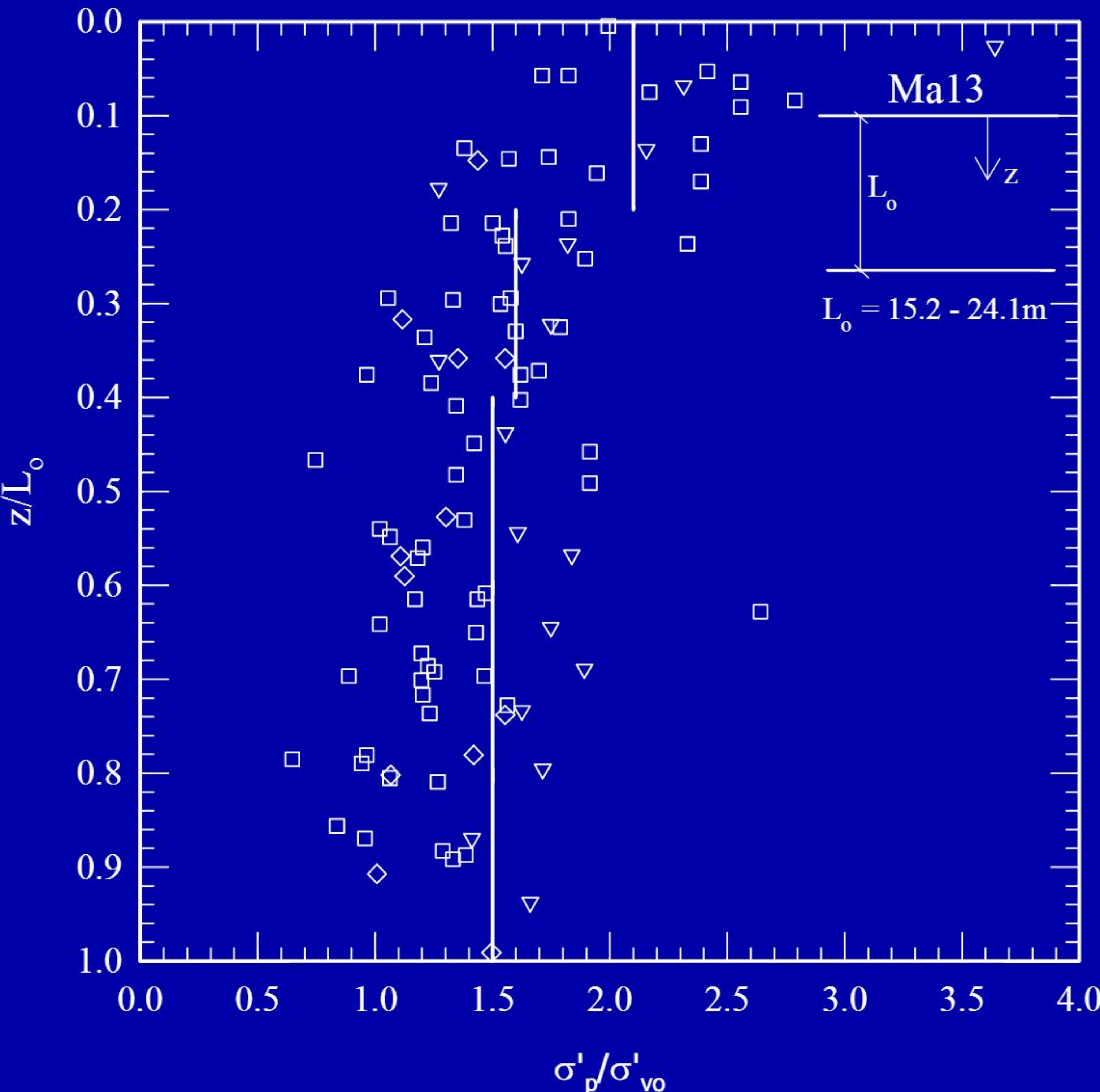

Ma13
z
L_o
L_o = 15.2 - 24.1m
z/L_o
σ'p/σ'vo
0.0
0.1
0.2
0.3
0.4
0.5
0.6
0.7
0.8
0.9
1.0
0.0
0.5
1.0
1.5
2.0
2.5
3.0
3.5
4.0

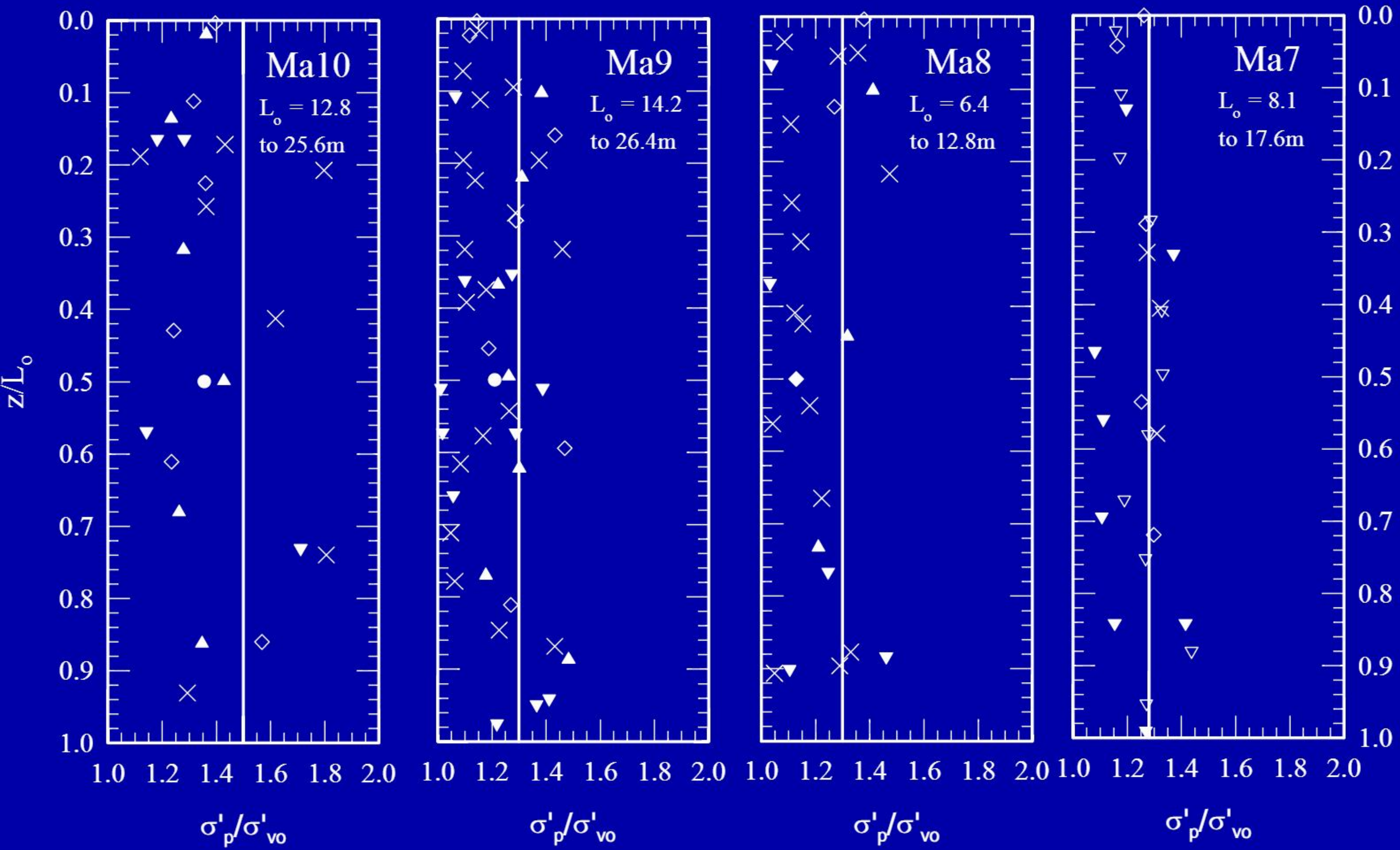

Ma10
L_o = 12.8 to 25.6m
Ma9
L_o = 14.2 to 26.4m
Ma8
L_o = 6.4 to 12.8m
Ma7
L_o = 8.1 to 17.6m
z/L_o
0.0
0.1
0.2
0.3
0.4
0.5
0.6
0.7
0.8
0.9
1.0
1.0
1.2
1.4
1.6
1.8
2.0
σ'_p/σ'_{vo}

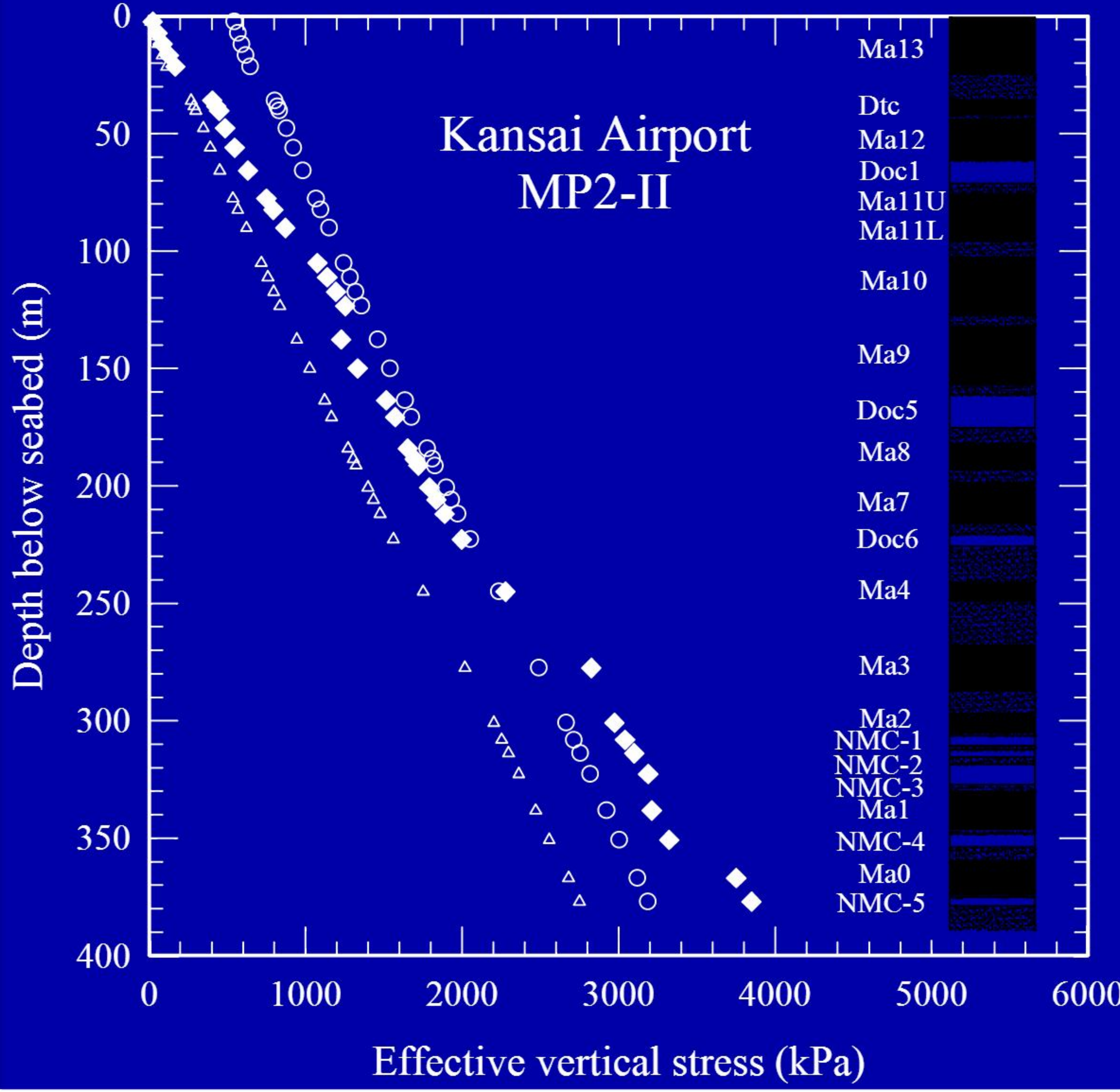
Kansai Airport
MP2-II
Depth below seabed (m)
Effective vertical stress (kPa)
0
50
100
150
200
250
300
350
400
0
1000
2000
3000
4000
5000
6000
Ma13
Dtc
Ma12
Doc1
Ma11U
Ma11L
Ma10
Ma9
Doc5
Ma8
Ma7
Doc6
Ma4
Ma3
Ma2
NMC-1
NMC-2
NMC-3
Ma1
NMC-4
Ma0
NMC-5

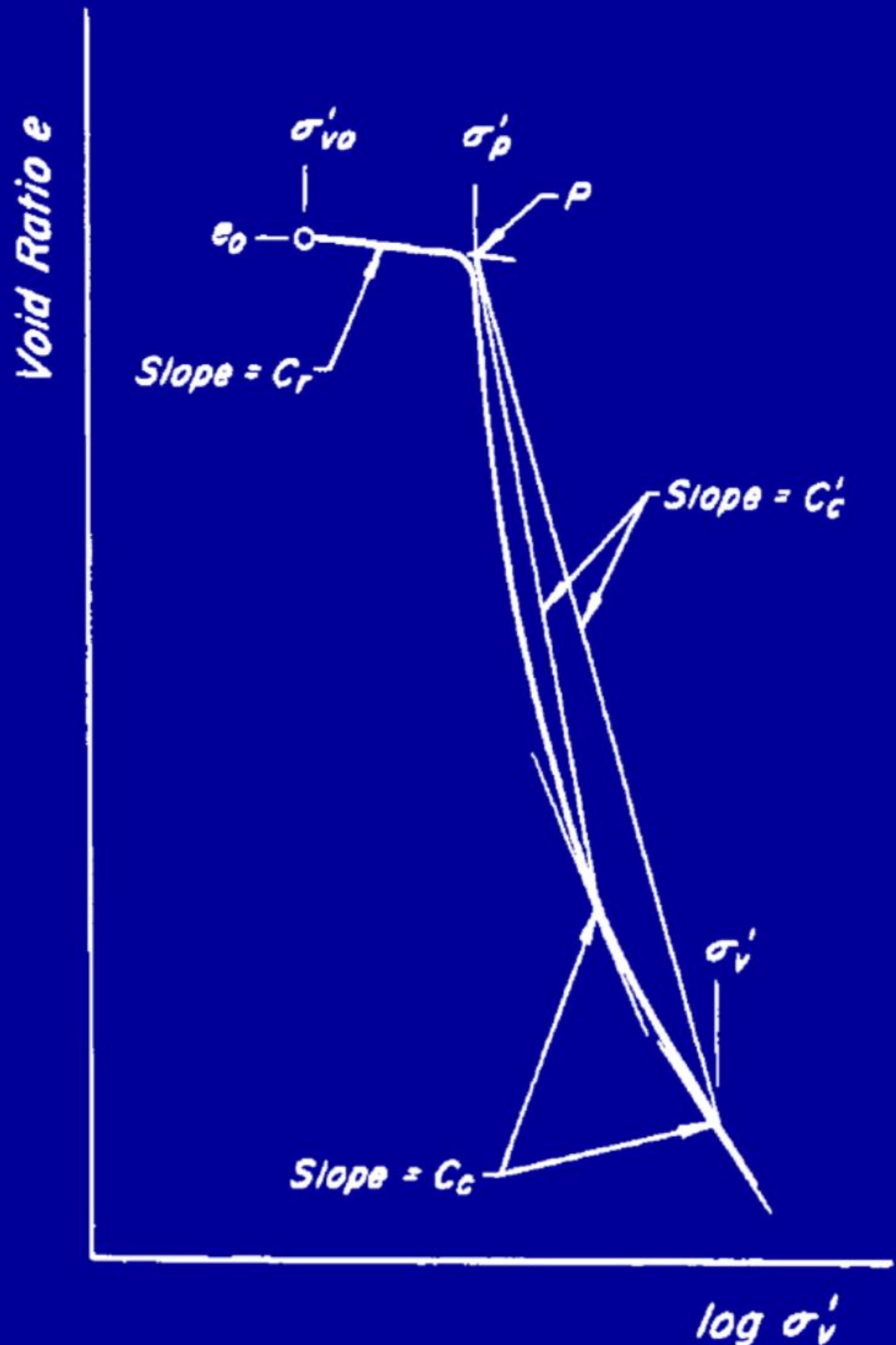

Void Ratio e
σ'vo
σ'p
P
e0
Slope = Cr
Slope = C'c
σ'v
Slope = Cc
log σ'v

Compressibility of Osaka Bay Clay Layers (cont.)

- The C'_c versus log σ'_v/σ'_p of the Holocene clay, and Pleistocene clay layers were obtained from incremental loading and constant rate of strain oedometer tests.

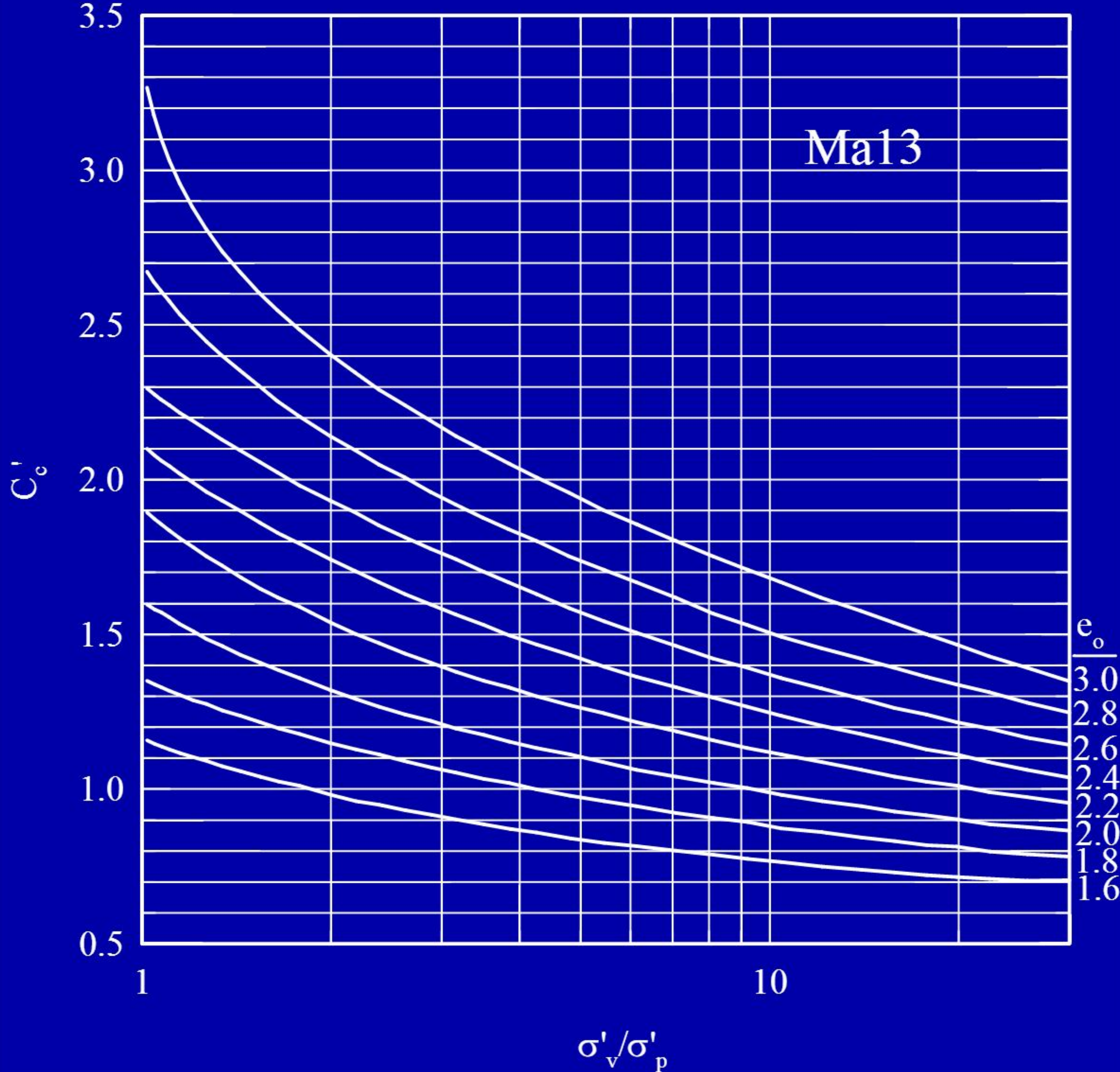
Ma13
C'c
σ'v/σ'p
e0
3.0
2.8
2.6
2.4
2.2
2.0
1.8
1.6
3.5
3.0
2.5
2.0
1.5
1.0
0.5
1
10

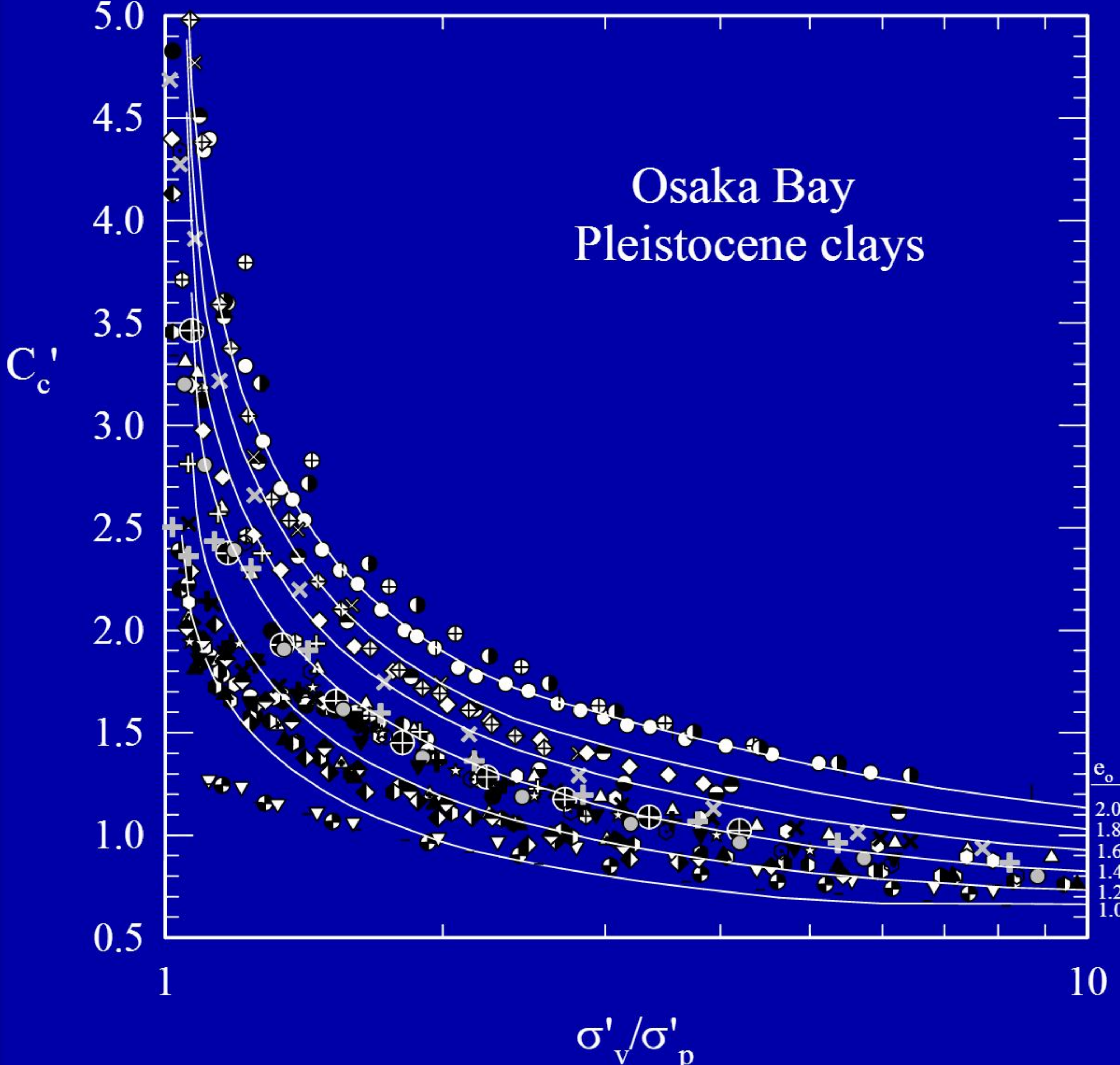

Osaka Bay
Pleistocene clays
Cc'
σ'v/σ'p
5.0
4.5
4.0
3.5
3.0
2.5
2.0
1.5
1.0
0.5
1
10
eo
2.0
1.8
1.6
1.4
1.2
1.0

Hydrodynamic Equation

- Holocene clay layer with vertical sand drains

$$\frac{de}{dt} = \frac{1}{\gamma_w}\left(\frac{1+e_o}{1+e}\right)^2 \left[(1+e)\left(k_z \frac{\partial^2 u'}{\partial z^2} + \frac{\partial k_z}{\partial z}\frac{\partial u'}{\partial z}\right) - k_z \frac{\partial u'}{\partial z}\frac{\partial e}{\partial z}\right]$$

$$+ \frac{1+e}{\gamma_w}\left[k_r\left(\frac{1}{r}\frac{\partial u'}{\partial r} + \frac{\partial^2 u'}{\partial r^2}\right) + \frac{\partial k_r}{\partial r}\frac{\partial u'}{\partial r}\right]$$

Hydrodynamic Equation (cont.)

- Pleistocene clay layers

$$\frac{de}{dt} = \frac{1}{\gamma_w}\left(\frac{1+e_o}{1+e}\right)^2\left[(1+e)\left(k_z\frac{\partial^2 u'}{\partial z^2} + \frac{\partial k_z}{\partial z}\frac{\partial u'}{\partial z}\right) - k_z\frac{\partial u'}{\partial z}\frac{\partial e}{\partial z}\right]$$

$$+\frac{1+e}{\gamma_w}\left[k_x\frac{\partial^2 u'}{\partial x^2} + \frac{\partial k_x}{\partial x}\frac{\partial u'}{\partial x}\right]$$

Hydrodynamic Equation (cont.)

- Horizontal flow in X direction only – the length to width ratio of the Islands more than 3.5

Constitutive Equation

- The EOP e – log σ'_v relation of each clay sublayer is input into computer.
- The C_α / C_c of each clay layer is input into computer.

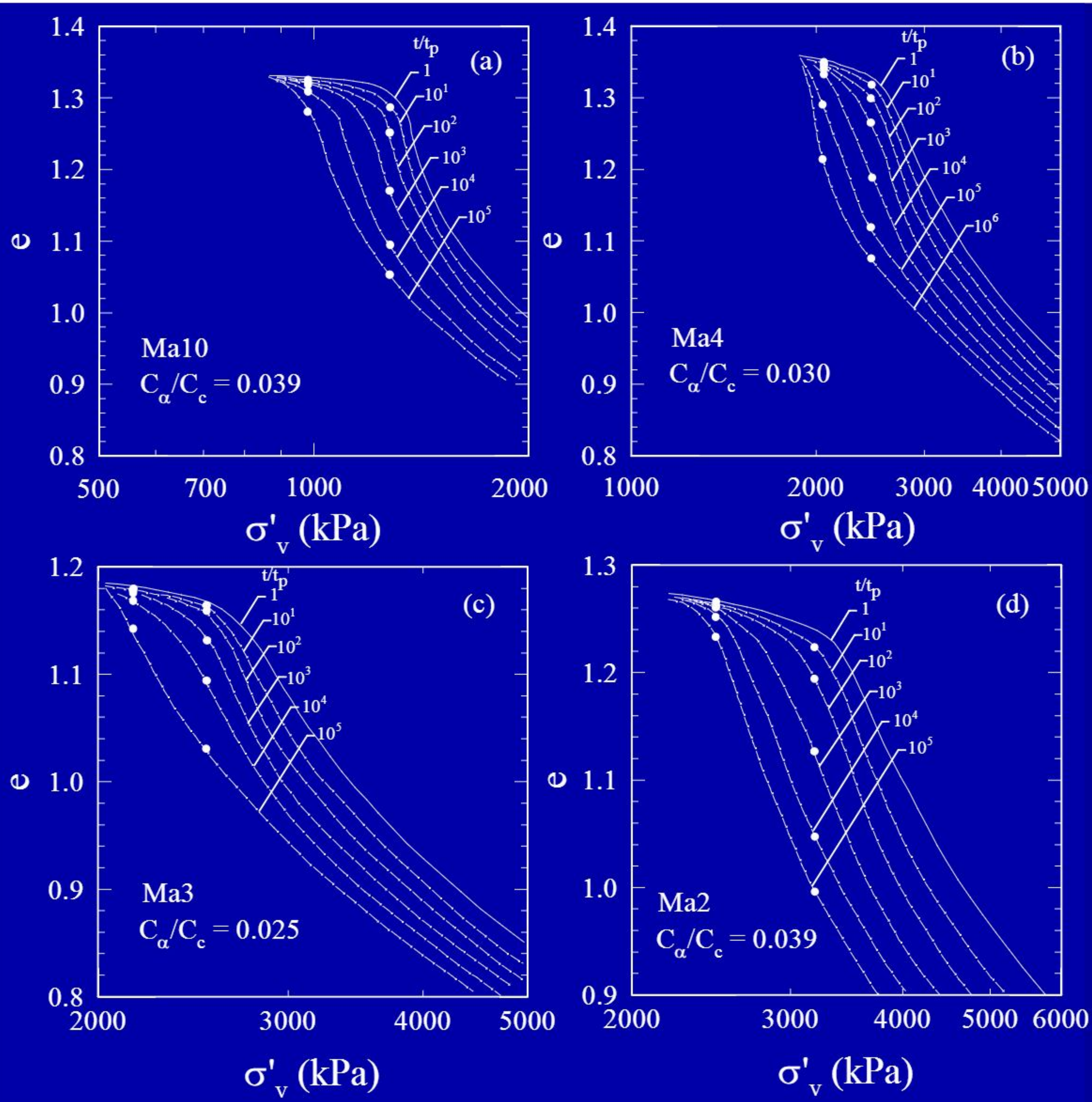

(a)
t/tp
1
10^1
10^2
10^3
10^4
10^5
Ma10
Cα/Cc = 0.039
e
σ'v (kPa)
(b)
t/tp
1
10^1
10^2
10^3
10^4
10^5
10^6
Ma4
Cα/Cc = 0.030
e
σ'v (kPa)
(c)
t/tp
1
10^1
10^2
10^3
10^4
10^5
Ma3
Cα/Cc = 0.025
e
σ'v (kPa)
(d)
t/tp
1
10^1
10^2
10^3
10^4
10^5
Ma2
Cα/Cc = 0.039
e
σ'v (kPa)

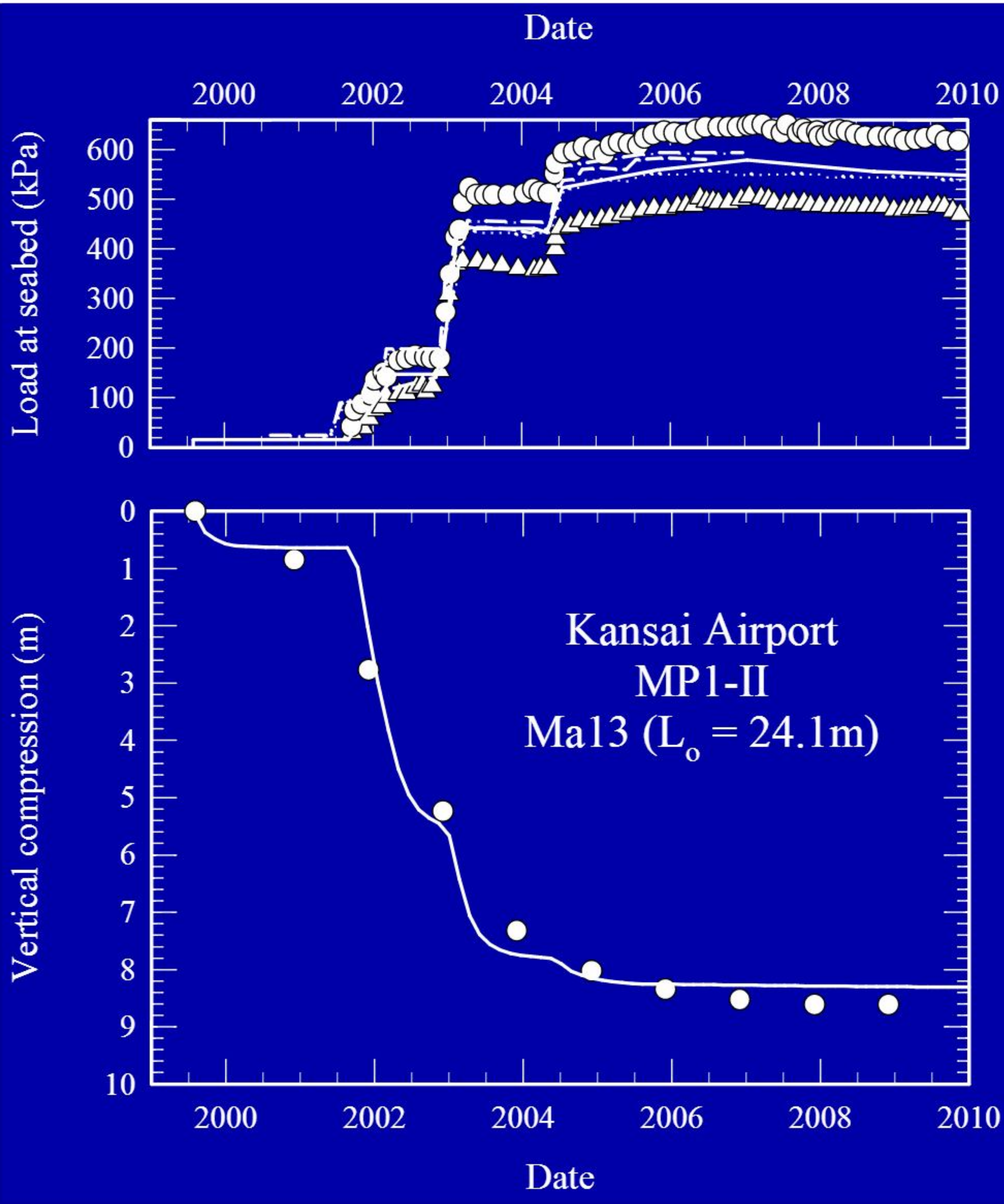
Date
2000
2002
2004
2006
2008
2010
Load at seabed (kPa)
0
100
200
300
400
500
600
Vertical compression (m)
0
1
2
3
4
5
6
7
8
9
10
Kansai Airport
MP1-II
Ma13 (L$_o$ = 24.1m)
Date

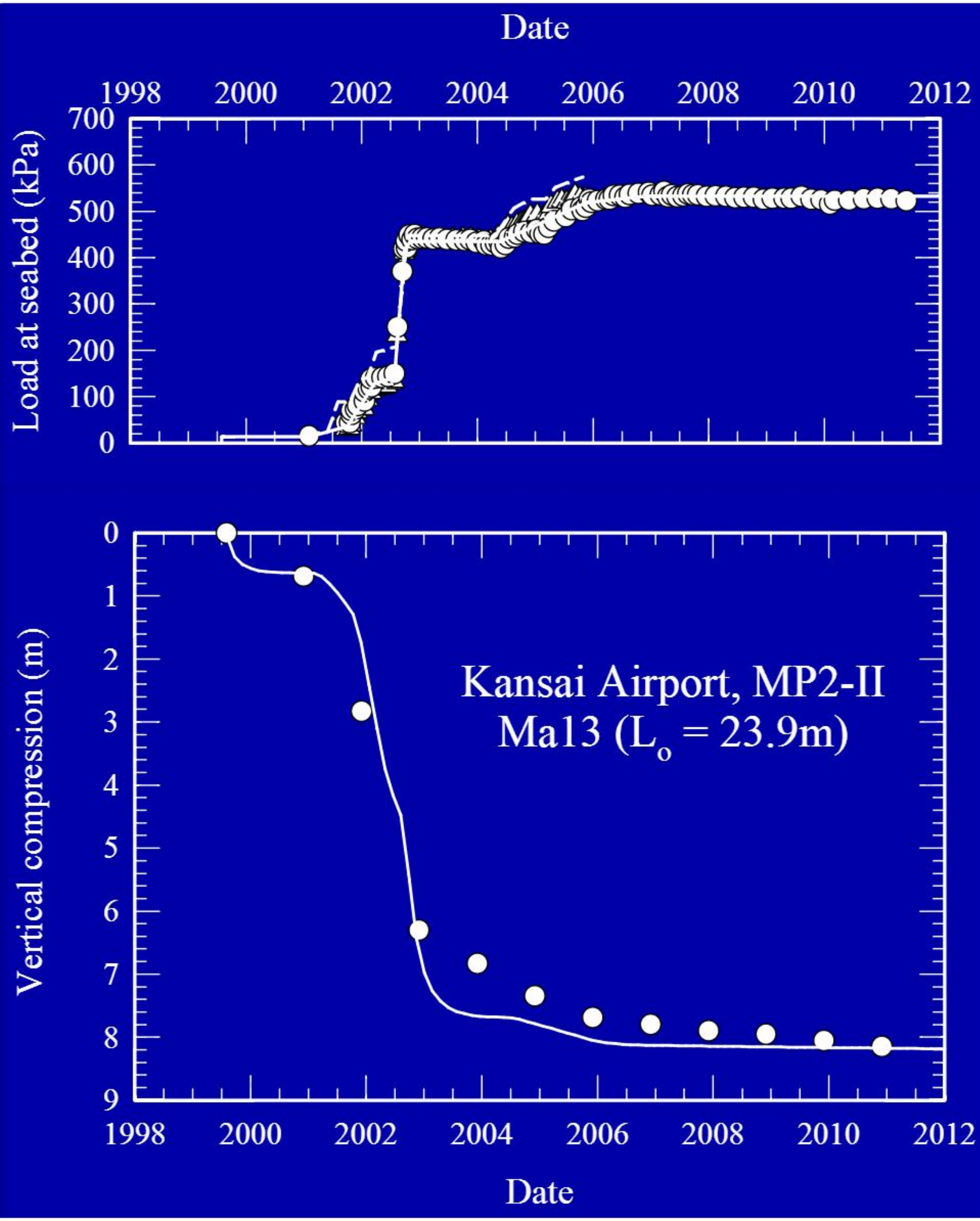

Date
1998
2000
2002
2004
2006
2008
2010
2012
Load at seabed (kPa)
0
100
200
300
400
500
600
700
Vertical compression (m)
0
1
2
3
4
5
6
7
8
9
Kansai Airport, MP2-II
Ma13 (Lo = 23.9m)

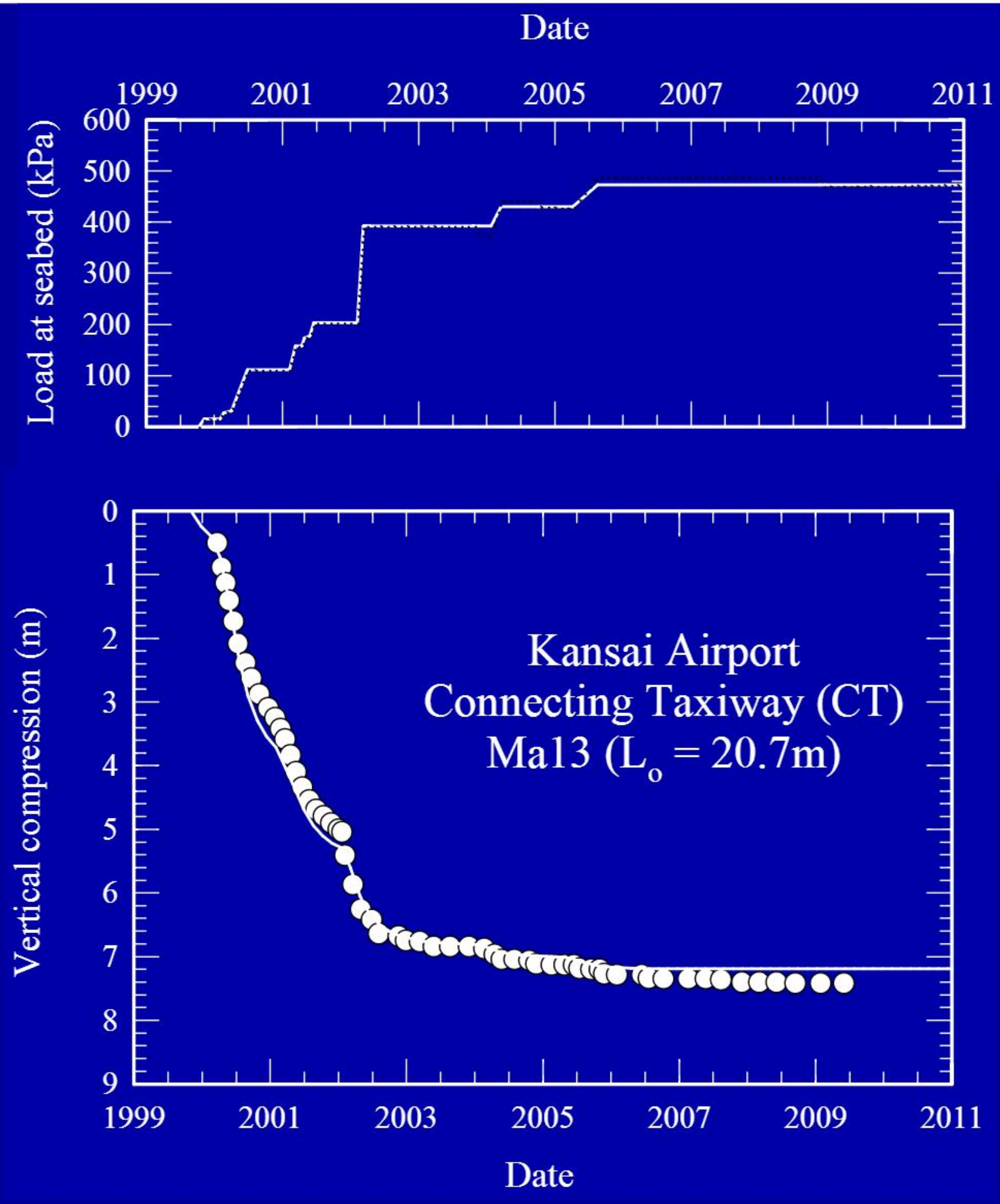

Date
1999
2001
2003
2005
2007
2009
2011
Load at seabed (kPa)
0
100
200
300
400
500
600
Vertical compression (m)
0
1
2
3
4
5
6
7
8
9
Kansai Airport
Connecting Taxiway (CT)
Ma13 (L$_o$ = 20.7m)
1999
2001
2003
2005
2007
2009
2011
Date

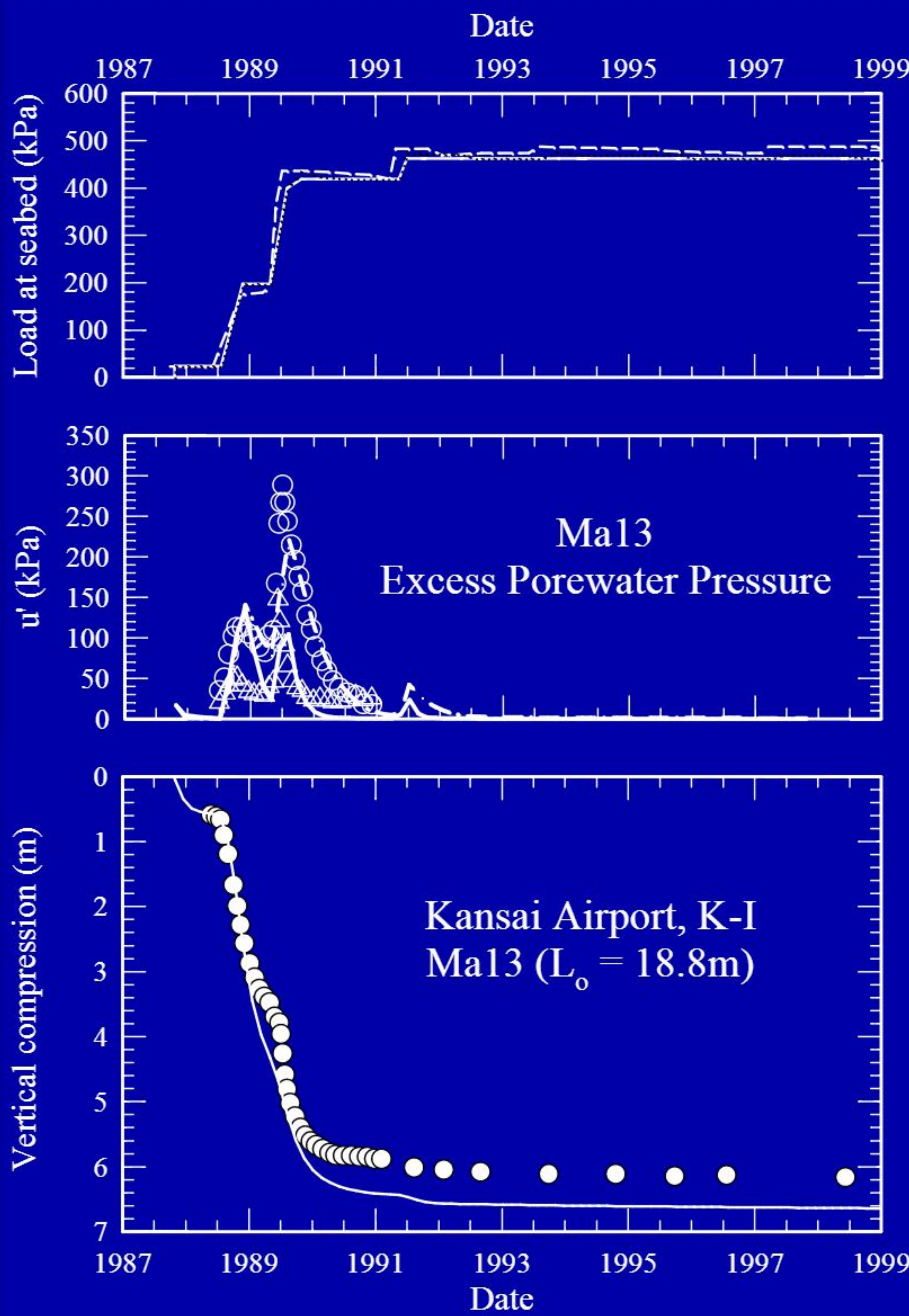

Date
1987
1989
1991
1993
1995
1997
1999
Load at seabed (kPa)
0
100
200
300
400
500
600
u' (kPa)
0
50
100
150
200
250
300
350
Ma13
Excess Porewater Pressure
Vertical compression (m)
0
1
2
3
4
5
6
7
Kansai Airport, K-I
Ma13 (L_o = 18.8m)

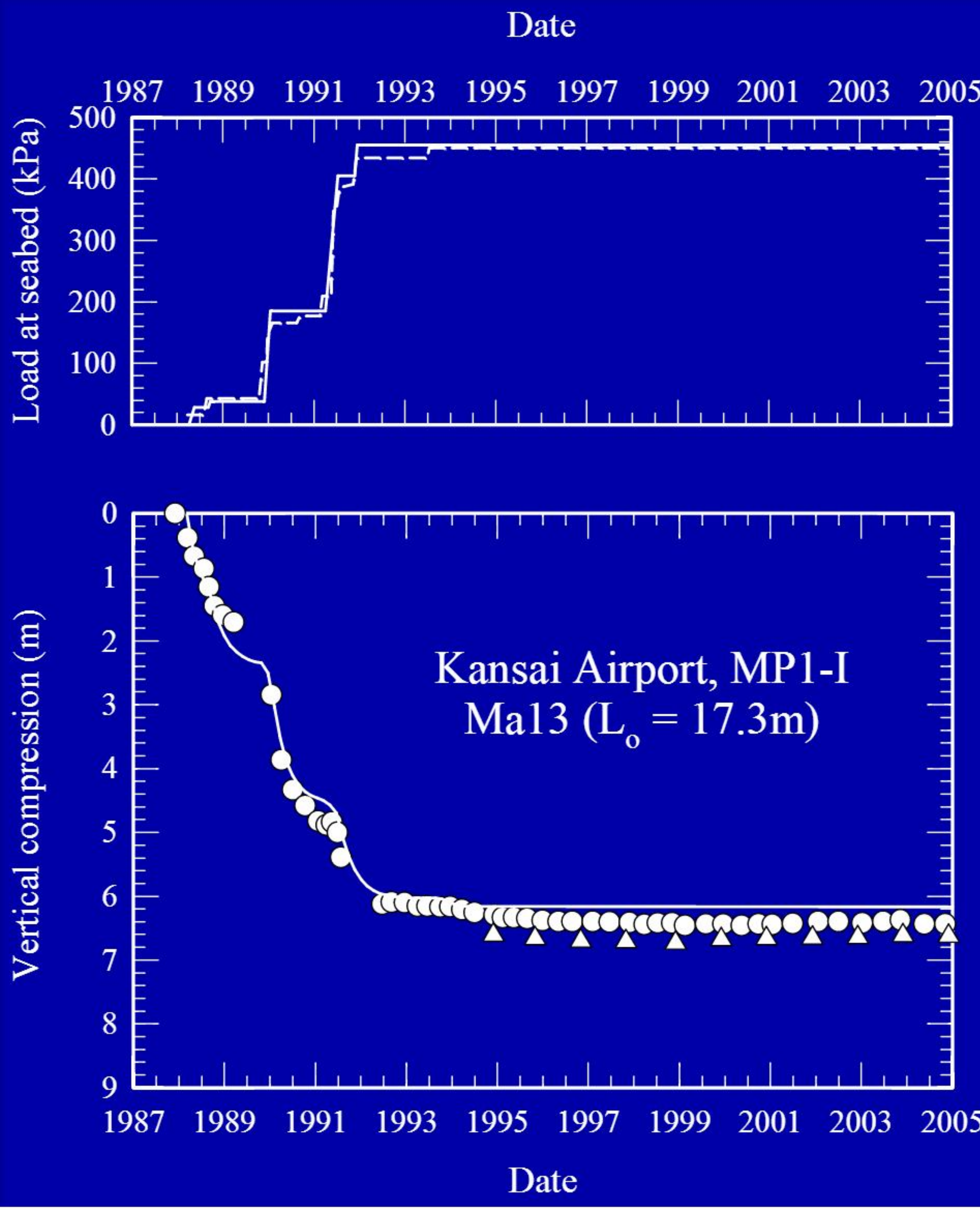

Date
1987
1989
1991
1993
1995
1997
1999
2001
2003
2005
Load at seabed (kPa)
500
400
300
200
100
0
Vertical compression (m)
0
1
2
3
4
5
6
7
8
9
Kansai Airport, MP1-I
Ma13 (L_o = 17.3m)
1987
1989
1991
1993
1995
1997
1999
2001
2003
2005
Date

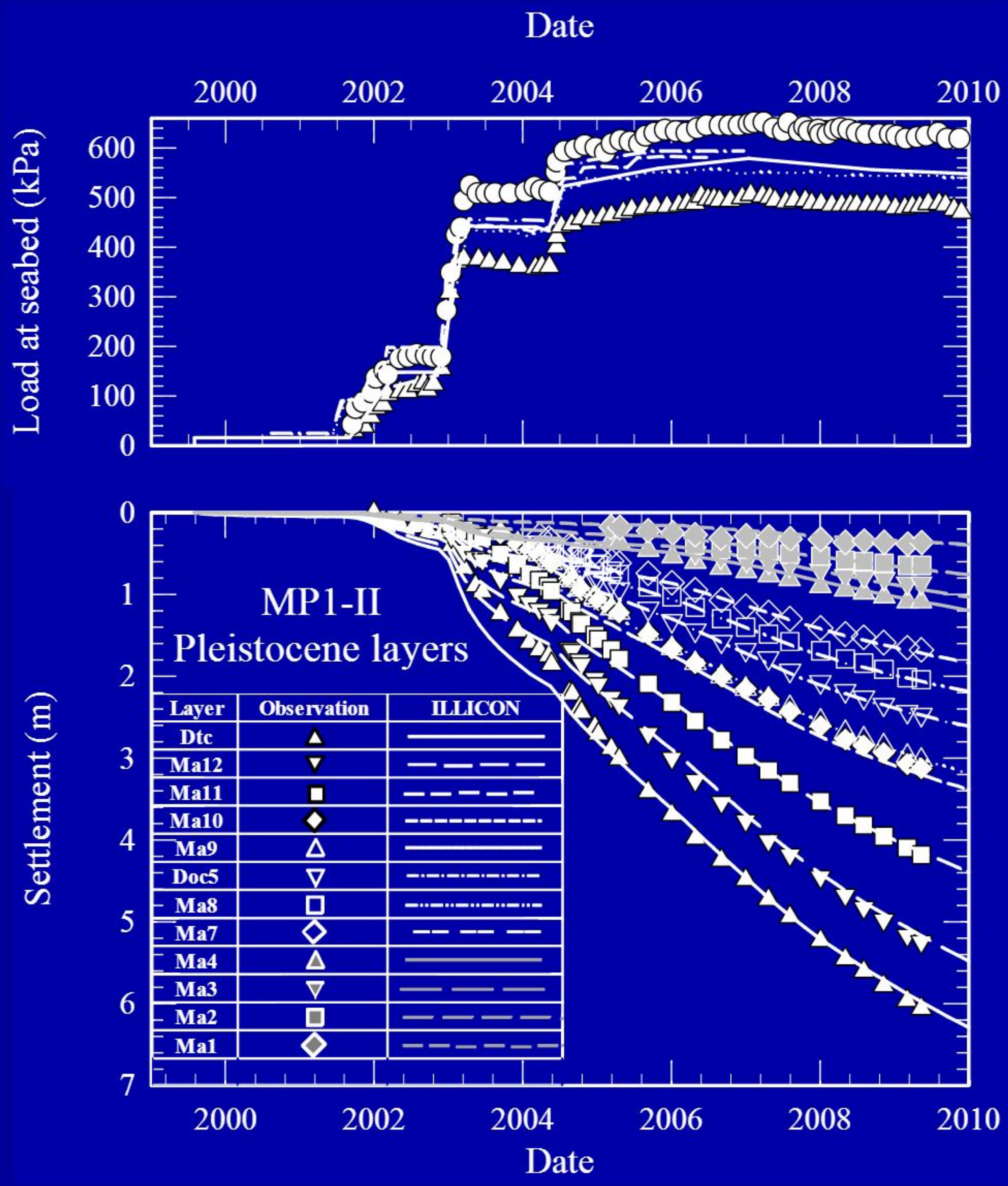

Date
2000
2002
2004
2006
2008
2010
Load at seabed (kPa)
0
100
200
300
400
500
600
MP1-II
Pleistocene layers
Settlement (m)
Layer
Observation
ILLICON
Dtc
Ma12
Ma11
Ma10
Ma9
Doc5
Ma8
Ma7
Ma4
Ma3
Ma2
Ma1

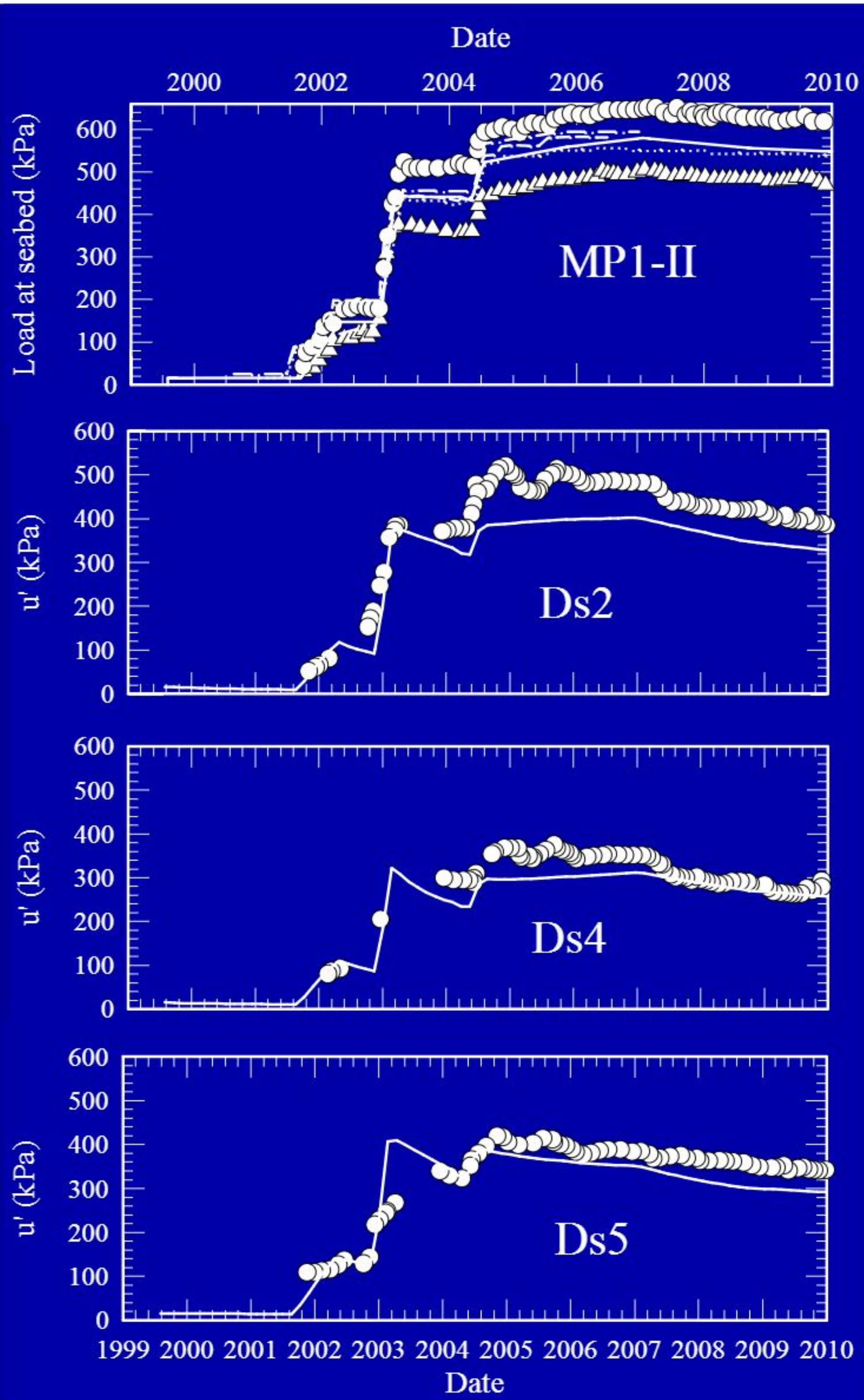
Date
2000
2002
2004
2006
2008
2010
Load at seabed (kPa)
0
100
200
300
400
500
600
MP1-II
u' (kPa)
Ds2
Ds4
Ds5
1999
2000
2001
2002
2003
2004
2005
2006
2007
2008
2009
2010
Date

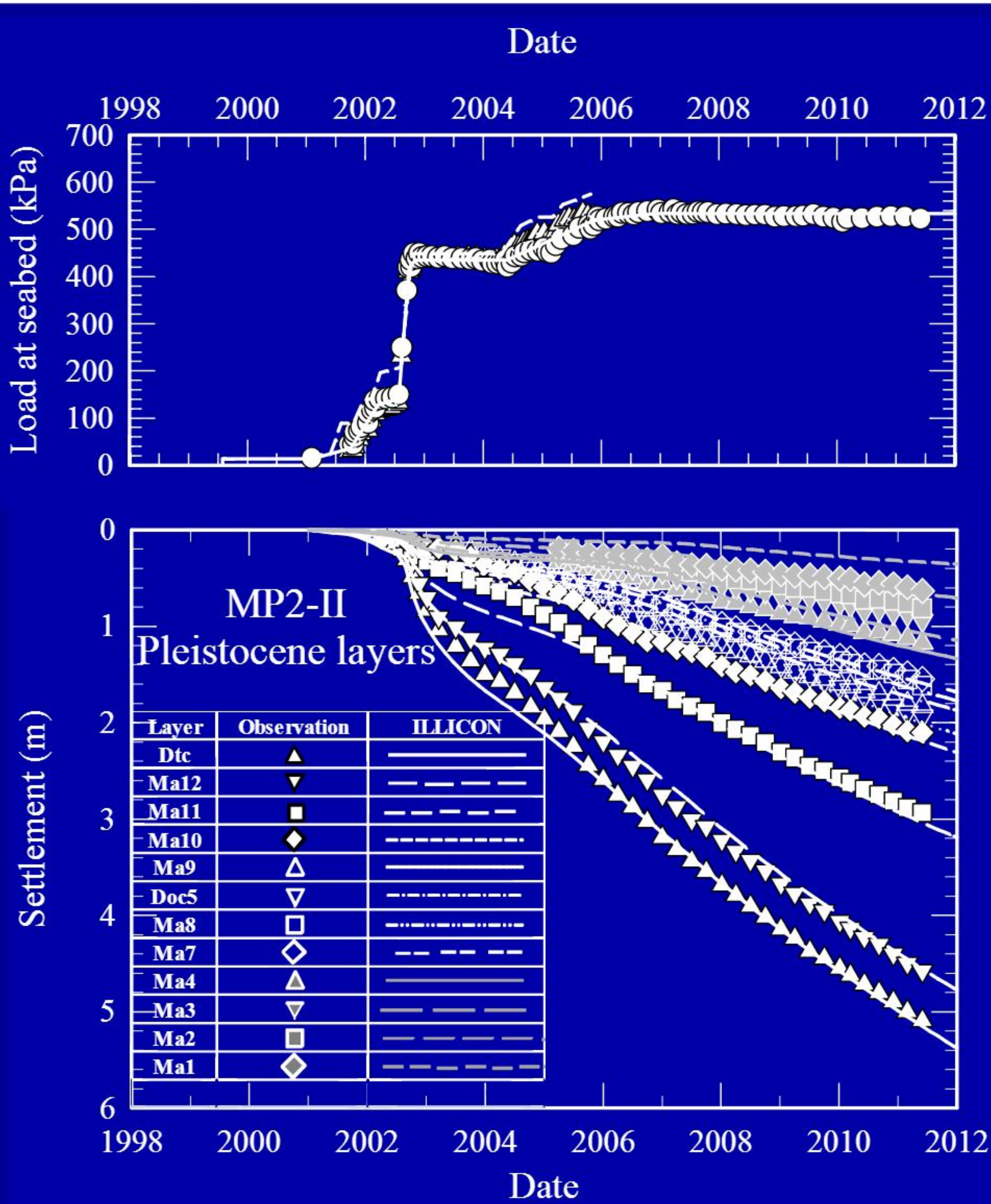
Date
1998 2000 2002 2004 2006 2008 2010 2012
Load at seabed (kPa)
0 100 200 300 400 500 600 700
Settlement (m)
0 1 2 3 4 5 6
MP2-II
Pleistocene layers
Layer | Observation | ILLICON
Dtc
Ma12
Ma11
Ma10
Ma9
Doc5
Ma8
Ma7
Ma4
Ma3
Ma2
Ma1

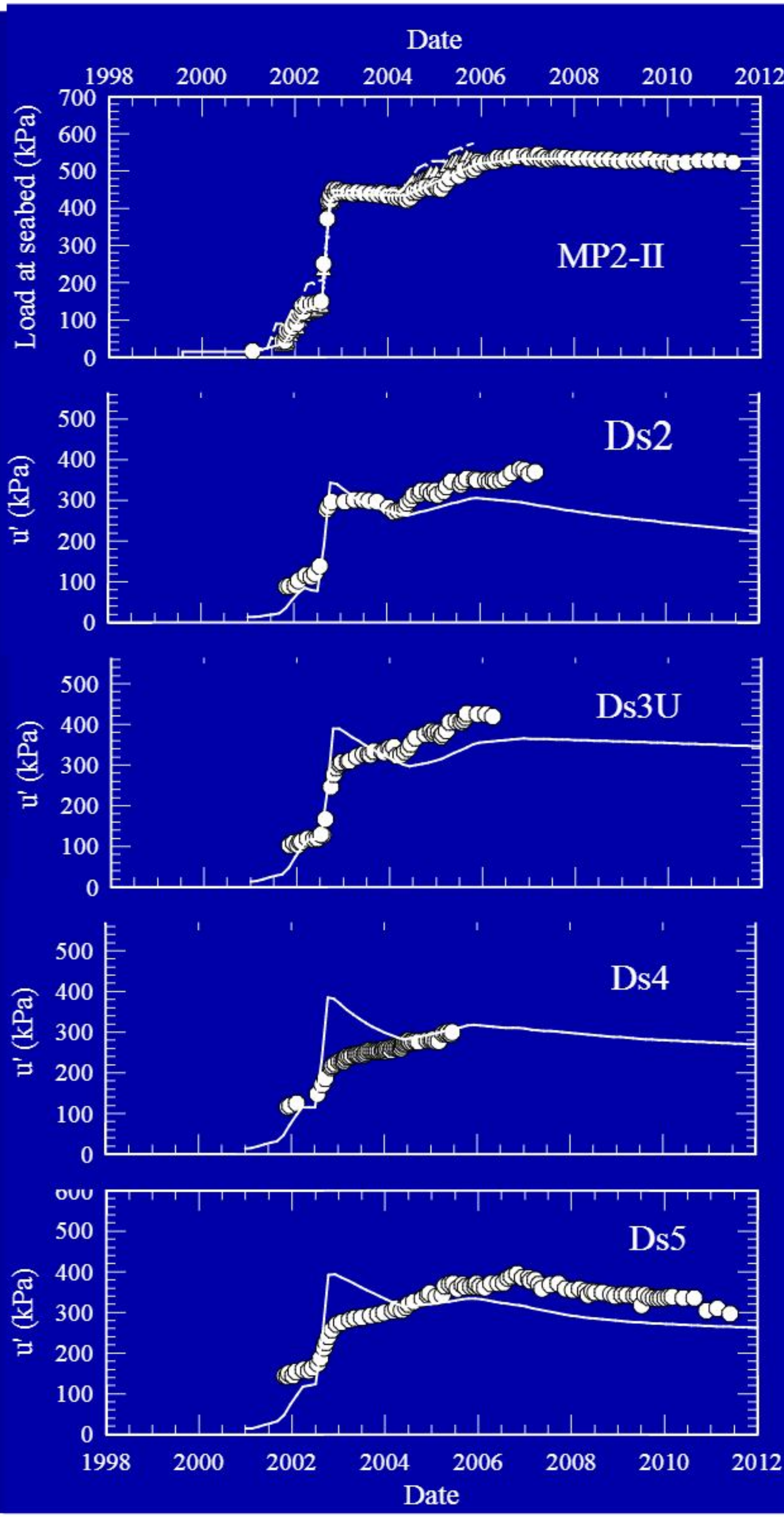

Date
Load at seabed (kPa)
MP2-II
u' (kPa)
Ds2
Ds3U
Ds4
Ds5
Date

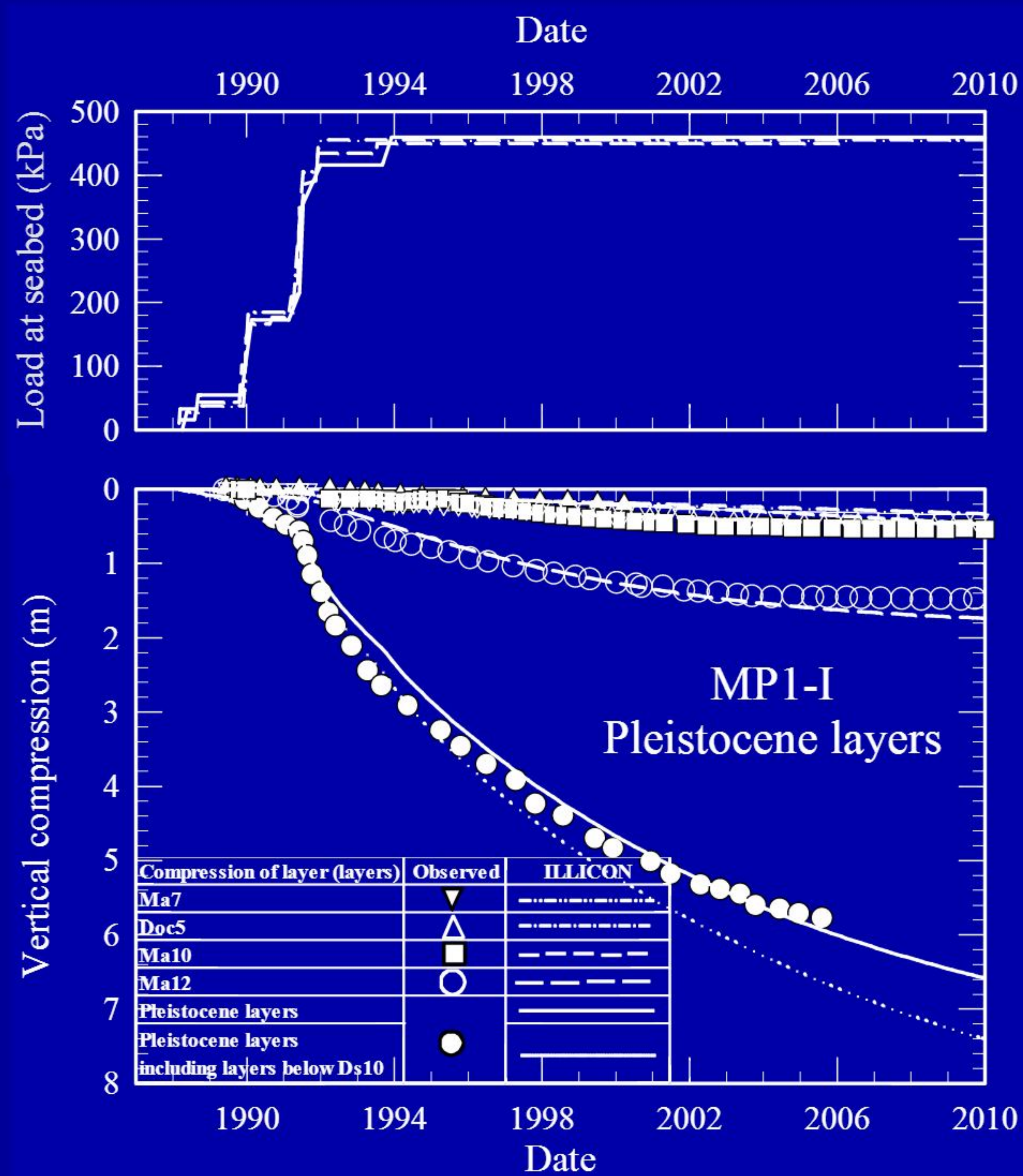

Date
1990
1994
1998
2002
2006
2010
Load at seabed (kPa)
500
400
300
200
100
0
Vertical compression (m)
0
1
2
3
4
5
6
7
8
MP1-I
Pleistocene layers
Compression of layer (layers)
Observed
ILLICON
Ma7
Doc5
Ma10
Ma12
Pleistocene layers
Pleistocene layers
including layers below Ds10
Date

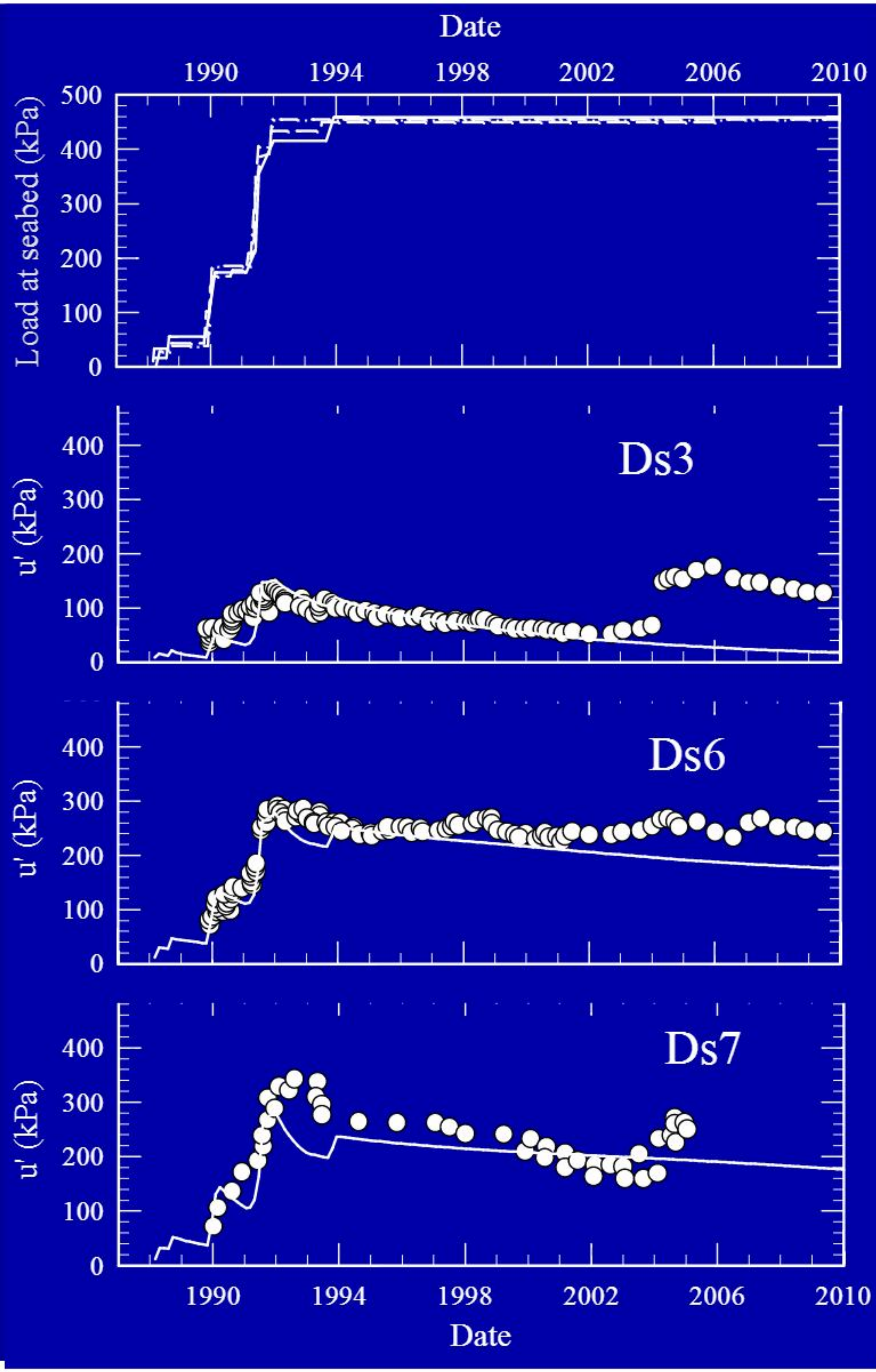

Date
1990
1994
1998
2002
2006
2010
Load at seabed (kPa)
0
100
200
300
400
500
Ds3
u' (kPa)
Ds6
u' (kPa)
Ds7
u' (kPa)
Date

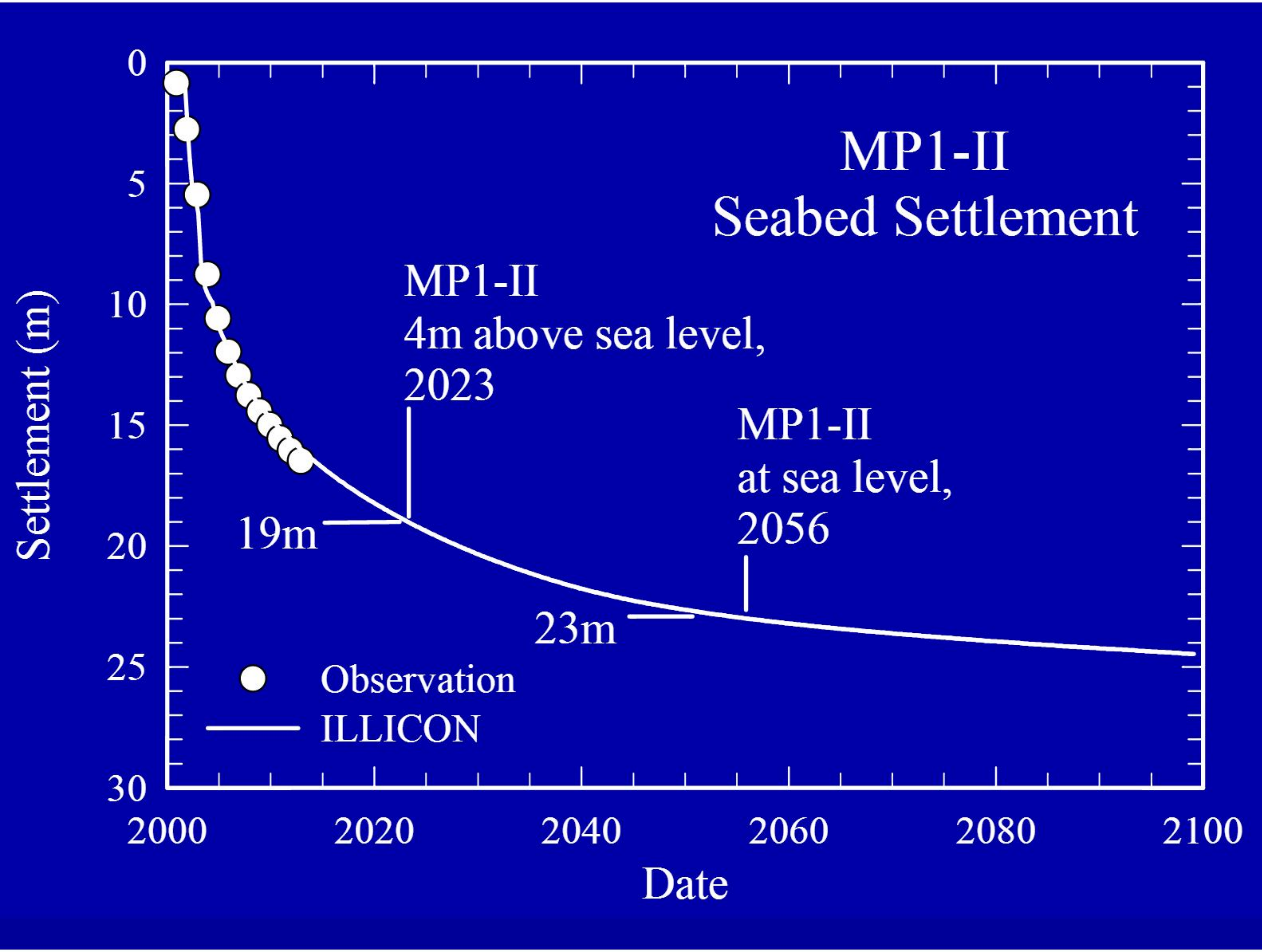
MP1-II
Seabed Settlement
MP1-II
4m above sea level,
2023
MP1-II
at sea level,
2056
19m
23m
Observation
ILLICON
Settlement (m)
0
5
10
15
20
25
30
2000
2020
2040
2060
2080
2100
Date

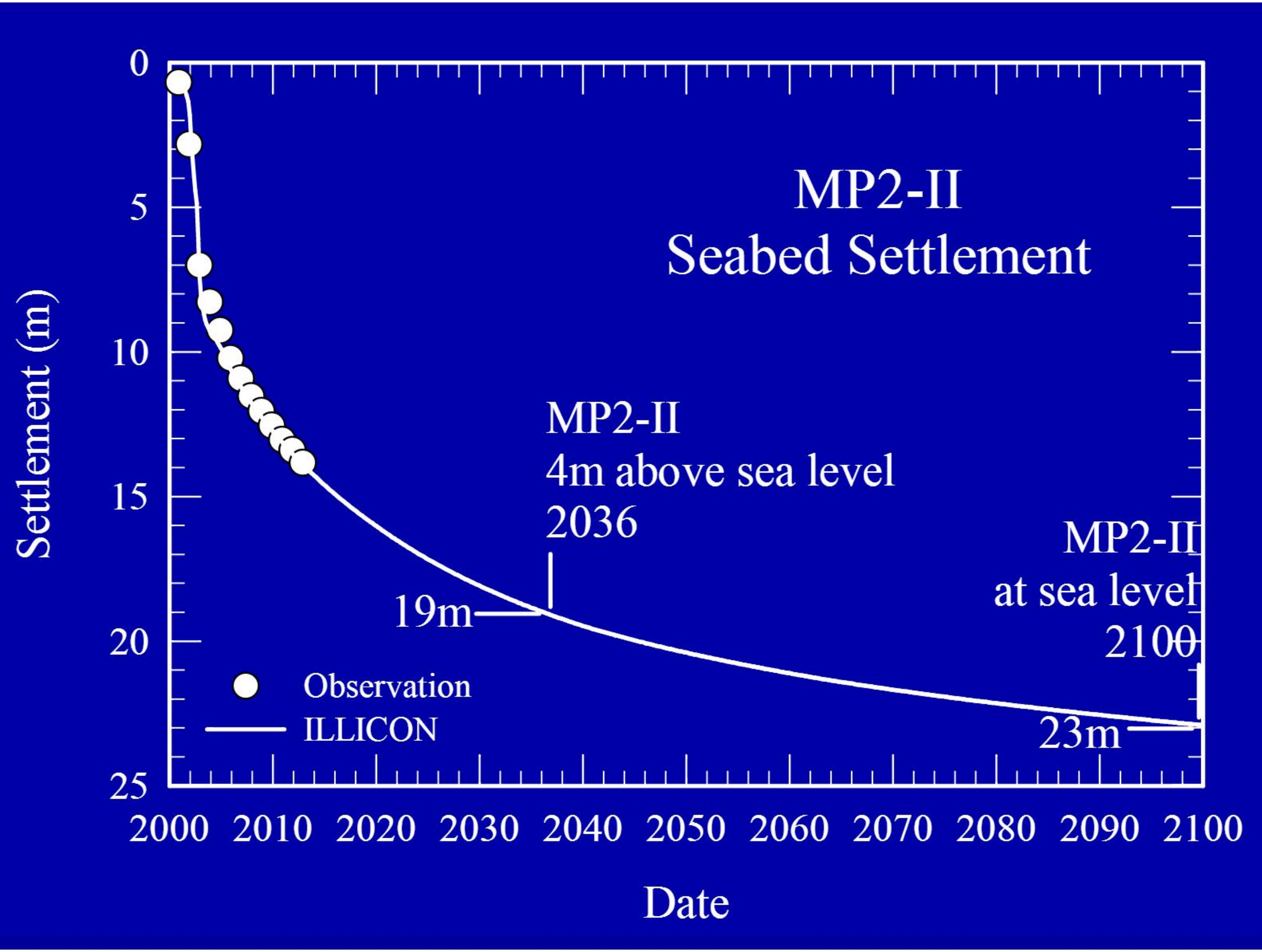
MP2-II
Seabed Settlement
Settlement (m)
0
5
10
15
20
25
Date
2000
2010
2020
2030
2040
2050
2060
2070
2080
2090
2100
MP2-II
4m above sea level
2036
19m
MP2-II
at sea level
2100
23m
Observation
ILLICON

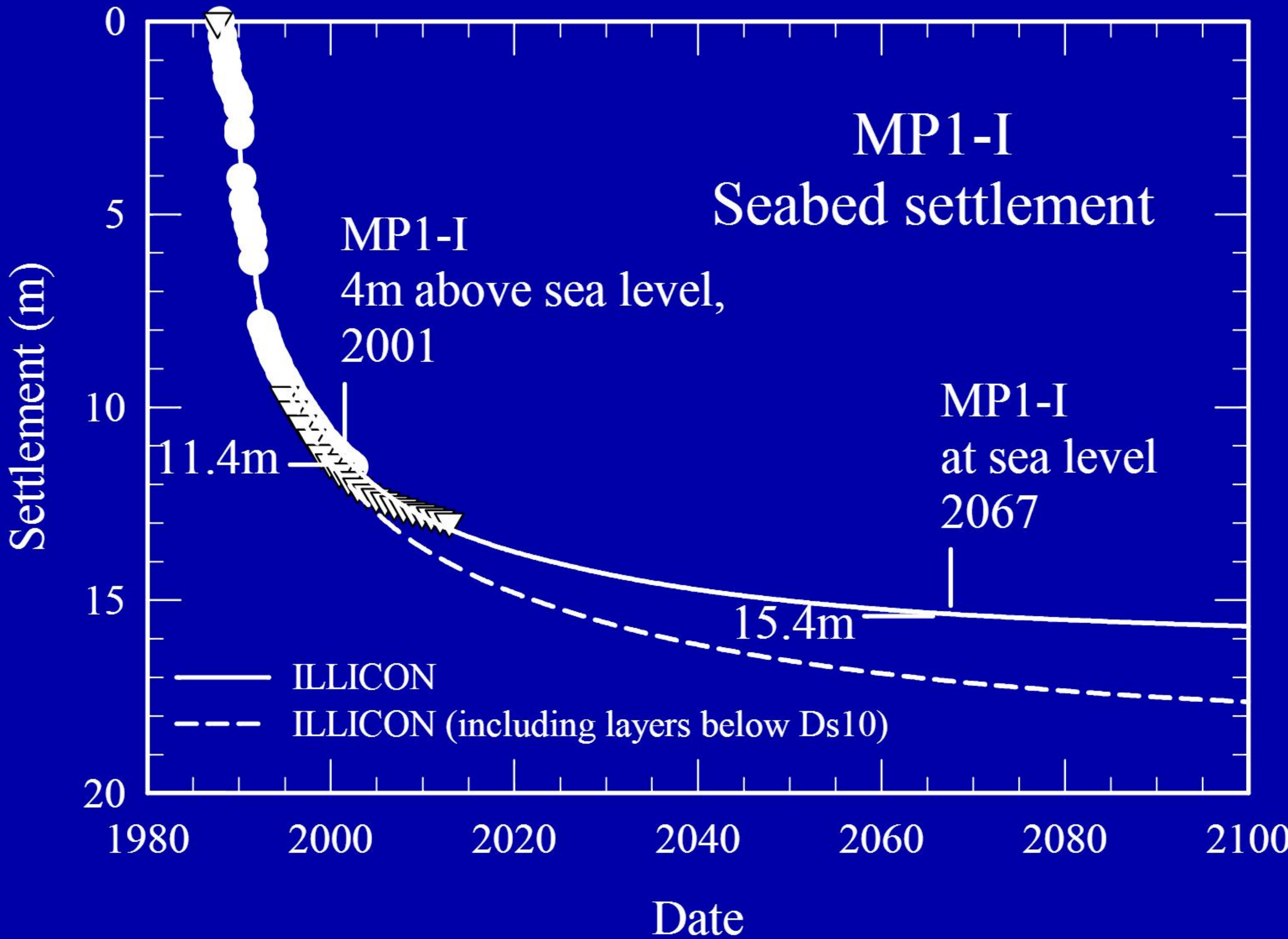
MP1-I
Seabed settlement
MP1-I
4m above sea level,
2001
MP1-I
at sea level
2067
11.4m
15.4m
ILLICON
ILLICON (including layers below Ds10)
Settlement (m)
0
5
10
15
20
1980
2000
2020
2040
2060
2080
2100
Date

Conclusions

1. The basement rock, located at depths of 1000 m at the Kansai Airport site, is overlain by an alternating sequence of Pleistocene marine and non-marine clay and sand layers with an overlying 17 m to 25 m thick Holocene marine clay layer. The upper 400 m of the subseabed profile at the airport site MP1-II consists of 22 clay layers with a combined thickness of 290 m and 19 sand layers with a combined thickness of 110 m. The lowermost Pleistocene clay layer was deposited 1 million YBP, and deposition of the Holocene clay layer began 10 to 12 thousand YBP.

Conclusions (cont.)

2. The pre-reclamation subseabed condition at the Kansai Airport site was defined by 63 borings made to depths of 100 m to 200 m below seabed, and 6 borings made to a depth of 400 m below seabed. Representative values of natural water content, plastic limit, liquid limit, clay-size fraction, and activity for 22 clay layers are in the range of 19 to 110%, 18 to 41%, 35 to 110%, 6 to 52%, and 0.99 to 3.04, respectively.

Conclusions (cont.)

3. For the ILLICON settlement analyses, vertical permeability of the Pleistocene clay layers in the range of $5x10^{-9}$ m/s to $8x10^{-11}$ m/s was calculated using the empirical equation by Mesri et al. (1994) together with representative values of pre-reclamation void ratio, clay-size fraction and activity for each sublayer. For all clay layers, the decrease in permeability during consolidation was calculated using the empirical equation $C_k = 0.5e_o$.

Conclusions (cont.)

4. The permeability of the Pleistocene sand layers was back-calculated using the ILLICON computer program together with settlement and porewater pressure observations, assuming horizontal flow within the sand layers. The back-calculated permeability values were in the range of 10^{-7} to 10^{-4} m/s which is comparable to values used in settlement analyses performed by others in the literature for the Kansai Airport islands.

Conclusions (cont.)

5. The compressibility of each clay sublayer was defined in terms of an EOP $e - \log \sigma'_v$ relationship together with a value of C_α/C_c. The EOP $e - \log \sigma'_v$ relationship of each sublayer started from the pre-reclamation point (e_o, σ'_{vo}) continued along a recompression curve assuming $C_r/C_c = 0.1$ to a preconsolidation pressure computed from σ'_p/σ'_{vo} data in the range of 1.28 to 2.10 for Holocene and Pleistocene clay layers, then to a non-linear compression curve constructed using $C_c' - \log \sigma'_v/\sigma'_p$ data from all published IL and CRS oedometer tests on Holocene and Pleistocene clays from the Kansai Airport site.

Conclusions (cont.)

6. The ILLICON computer program was rebuilt especially to accommodate the Pleistocene sand layers in the Osaka Bay subseabed as incompressible impeded drainage boundaries that discharge water in the horizontal direction, perpendicular to the long dimension of each airport island.

Conclusions (cont.)

7. Computed EOP compression of Ma13 is 5.8 m at MP1-I, 8.1 m at MP2-II, and 8.3 m at MP1-II. According to observations and ILLICON analyses, primary consolidation of the Holocene Ma13 clay layer was realized soon after reclamation was completed in each location because of the presence of vertical drains. As of December 2012, the average observed seabed settlement has been 13.0 m and 14.6 m, respectively, for Airport Island I and II.

Conclusions (cont.)

8. According to the ILLICON analyses, by the end of the 21st century, MP1-I on Island I will settle 17.6 m and MP1-II and MP2-II on Island II will settle 24.4 m and 22.9 m, respectively.

Conclusions (cont.)

9. At MP1-II, 185 m combined thickness of clay (Ma13 to Doc6) was loaded to the compression range with maximum σ'_{vf}/σ'_p in the range of 1.05 to 2.15, and has experienced significant primary compression. On the other hand, 102 m combined thickness of Pleistocene clay was loaded to the recompression range with maximum σ'_{vf}/σ'_p in the range of 0.83 to 1.01, and because of the short duration of primary consolidation together with rapid increase in C_α with time, is expected to experience significant secondary compression.

Conclusions (cont.)

10. Airport Island I exceeded in 2001 the design specification requiring that the surface elevation of the airport islands should remain “4 m above sea level”. By 2067 or sooner Island I is predicted to be at sea level. The surface elevation of Airport Island II is predicted to be at the design requirement “4 m above sea level” by 2023 to 2036, and Airport Island II is predicted to be at sea level by 2058 to 2100.

Conclusions (cont.)

11. According to the ILLICON predictions, 100 years after construction of Airport Island II, the degree of primary compression of the 24.5 to 25.6 m thick Ma10 Pleistocene clay layer with impeded drainage boundaries will be 54 to 57%.